

Department of Electrical and Computer Systems Engineering

Technical Report MECSE-1-2007

Fiber Raman Amplification in Ultra-high Speed Ultra-long
Haul Transmission: Gain Profile, Noises and Transmission
Performance

L.N. Binh, T.L huynh, S. Sargent and A. Kirpalani

MONASH
UNIVERSITY

FIBER RAMAN AMPLIFICATION IN ULTRA-HIGH SPEED ULTRA-LONG HAUL TRANSMISSION: GAIN PROFILE, NOISES AND TRANSMISSION PERFORMANCE

L.N. Binh, T.L. Huynh, S. Sargent and A. Kirpalani
Department of Electrical and Computer Systems Engineering, Monash
University, Clayton Campus, Victoria 3168 Australia

TECHNICAL REPORT
OPTICAL COMMUNICATIONS AND APPLIED PHOTONICS GROUP
CENTRE FOR TELECOMMUNICATIONS AND INFORMATION
ENGINEERING

TABLE OF CONTENTS

1 INTRODUCTORY REMARKS 0

2 LUMPED AND DISTRIBUTED AMPLIFYING SYSTEMS 1

3 RAMAN AMPLIFICATION PROCESSES 2

4.1 RAMAN AMPLIFICATION OPERATIONAL PRINCIPLES 2

4.2 SIGNAL AND PUMP COUPLED EQUATIONS 3

4.3 RAMAN SCATTERING NOISE 4

Spontaneous Raman Scattering 4

Rayleigh Backscattering 4

Fast response time due to short upper state lifetime 4

Noise Figure 4

4.4 LINEAR AND NON-LINEAR DISPERSION 4

Group Velocity Dispersion (GVD) 5

Fibers for distributed Raman amplification 5

4 NUMERICAL MODELING OF THE COUPLED EQUATIONS..... 6

4.1 GAIN 6

4.2 DISTRIBUTED GAIN 7

4.3 GAUSSIAN PULSE PROPAGATION 8

4.4 NOISE FIGURE 9

4.5 DISPERSION 10

4.6 DISCRETE RAMAN AMPLIFICATION 10

5 NON-LINEAR RAMAN GAIN/SCATTERING SCHRÖDINGER EQUATION 12

5.1 FIBER NONLINEARITIES 12

5.1 DISPERSION 13

5.3 SPLIT-STEP FOURIER METHOD 13

6. RAMAN OPTICALLY AMPLIFIED GAUSSIAN PULSES AND TRANSMISSION PERFORMANCE 13

Bi-Directional Pumping Case 15

Forward Pumping Case 16

Backward Pumping Case 16

6. ASK OPTICAL SYSTEM TRANSMISSION 16

Back to back performance 16

Transmission fiber but no amplification (Passive Fiber) 17

ASK with fiber Amplification random pulse sequence as compared to Gaussian single pulse 17

Transmission span integrated with EDFA Over 99km SSMF +DCF (1km Mismatch) 18

Distributed Raman Amplification 1 km SMF mismatched 100 km span 19

Bit Error Rates 19

Hybrid EDFA-ROA transmission 19

Multi-span transmission 20

8 CONCLUDING REMARKS 20

9. REFERENCES..... 21

LIST OF FIGURES

Figure 1 Lumped vs. distributed signal power evolution.	1
Figure 2: Multiple pump sources arrangement for Raman amplification in DWDM transmission. Operating band: 1530–1565 nm, Raman pump: multiplexed semiconductor lasers, Pump power up to 500 mW, Gain ripple: 0.8 dB, Small signal gain: 11 dB; OSNR improvement: 4.5 dB; PMD: 0.2 ps, PDG: 0.1 dB.....	1
Figure 3: Scattering caused by energy transitions of molecules into excited vibrational states.	2
Figure 4: Raman gain spectrum for fused silica [1].....	3
Figure 5: The schematic arrangement of the bidirectional pumping ROA.....	3
Figure 6: The Theoretical signal evolution using with percentages of forward pumping.....	4
Figure 7: Double Rayleigh Scattering.....	4
Figure 8 Measured Raman gain efficiency of different installed transmission optical fibers.	5
Figure 9 Effective Raman Gain co-efficient versus shifting frequency for NZ-DSF fiber.	6
Figure 10: Total Raman gain versus Stoke shift frequency for NZ-DSF.....	7
Figure 11: Gain over the Raman bandwidth.	7
Figure 12: The power evolution of the pump along the total length of the Corning NZ-DSF fiber for forward, backward and bi-directional configurations, blue, magenta and cyan respectively.....	7
Figure 13: The power evolution of the signal along the total length of the fiber for forward, backward and bi-directional configurations, blue, magenta and cyan respectively. The red line represents a passive fiber with no gain, $\alpha = 0.19\text{dB/km}$	7
Figure 14: The gain evolution over the total length of the fiber due to Raman amplification for forward, backward and bi-directional configurations.	8
Figure 15: The power evolution of the signal along the total length of the fiber with and without the effects of pump depletion, blue and green respectively.....	8
Figure 16: The power evolution of the pump along the total length of the fiber with and without the effects of pump depletion, blue and green respectively.....	8
Figure 17: The noise power associated with the signal along the total length of the fiber for forward, backward and bi-directional configurations.	9
Figure 18: Noise Figure versus on-off Raman gain for backward pumping case and investigating practical and ideal configurations.	9
Figure 19: Noise figure versus on-off Raman Gain for a 100km fiber varying input pump power using Corning NZ-DSF.	9
Figure 20: Noise Figure versus backward pumping ratio for different fibers over a 100km transmission link.	10
Figure 21 NF of Raman OA versus the optical gain in hybrid AEDFA+ ROA.....	10
Figure 22: Attenuation map of a passive fiber over the total length without amplification, $\alpha = 0.19\text{dB/km}$	11
Figure 23: The signal power evolution of a discrete Raman amplifier in the forward configuration.	11
Figure 24: Discrete Raman amplifier signal evolution for forward and backward configurations with $P_{S0}=0.1\text{mW}$ and equivalent theoretical results inserted (Headley, C & Agrawal, 2005)[1].....	11
Figure 25: NF versus fiber length for forward and backward pumping discrete Raman amplifiers.	11
Figure 26: Net Gain versus initial signal powers for different gain efficiencies.	12
Figure 27: The Span in Closer View by the SSFM [G.P. Agrawal, 'Nonlinear Fiber Optics'] [3].....	13
Figure 28: (a) Fluctuating Signal at Receiver and (b) Gaussian probability density.....	14
Figure 29 The power evolution of the signal along the total length of the fiber.....	14
Figure 30: The gain evolution over the total length of the fiber due to Raman amplification.	15
Figure 31: Gaussian Pulse Before and After Transmission.....	15
Figure 32: Signal Power Evolution: Bi-Directional Pumping.....	15
Figure 33: Gaussian: Bi-Directional Pumping.....	15
Figure 34: Signal Power Evolution: Forward Pumping.....	16
Figure 35: Gaussian: Forward Pumping.....	16
Figure 36: Evolution of the Signal Power under Backward Pumping.....	16
Figure 37: Gaussian pulses under Forward Pumping.....	16
Figure 38: Input Signal from the ASK Transmitter.....	17
Figure 39: Output Signal at the ASK Receiver.....	17
Figure 40: Gaussian: 3km Passive Fiber.....	17
Figure 41: Input Signal from the ASK Transmitter (Passive Fiber).....	17
Figure 42: Output Signal at the ASK Receiver (Passive Fiber).....	17
Figure 43: Signal Power Evolution: Forward Pumping.....	17
Figure 44: Gaussian: 3km Forward Pumped Fiber.....	18
Figure 45: Output Signal at the ASK Receiver (Forward Pumped).....	18
Figure 46: Input Signal at the ASK Transmitter (EDFA only).....	18
Figure 47: Output Signal of ASK Model (20dB gain EDFA only).....	18
Figure 48: Output Signal of ASK Model (9.5dB gain EDFA only).....	19
Figure 49: Output Signal of ASK Model (DRA model).	19
Figure 50: Output Signal of ASK Model (Hybrid model).	19
Figure 51 System simulation arrangement of a 4-span DWDM hybrid EDFA/ROA transmission 40Gb/s CS-RZ transmission system of 120 km /span.	20

Figure 52 Transmission span expansion 4-span 40Gb/s CS-RZ transmission system of 120 km /span (a) without Raman OA (b) with one Raman OA in one span. 20

Figure 53 Received eye diagrams of the transmission of random bit pattern over transmission span expansion 4-span 40Gb/s CS-RZ transmission system of 120 km /span with one Raman OA in one span..... 20

Summary

Optical transmission system design issues such as mid-span optically amplified distance, bandwidth enhancement can be assisted using Raman optical amplification (ROA) technology. ROA does not suffer from the limitations of EDFA in that it can be integrated with the transmission fibers, and pumped at any wavelength to provide wide gain bandwidth and gain flatness by employing a combination of different wavelength pumping sources. Different pumping configurations provide flexibility in the system for both distributed and discrete ROA. Only recently has ROA technology in transmission of optical signals become an achievable possibility, it offers a number of possible technical advancements to optically amplified long haul transmission infrastructure.

This paper thus investigates the Raman amplification in the transmission fibers including (i) the physical properties and operational characteristics and (ii) its implementation in the lightwave modulated envelop propagation equations, NLSE for transmission of 40 Gb/s signals in DWDM optical systems.

This study can thus be summarized as follows:

- *Development of numerical techniques based on using MATLAB programming platform to solve the coupled wave equations to obtain these design parameters for a single channel bi-directionally pumped system operating in the C-band spectrum.*
- *Investigations of Raman amplification of different transmission fibers for the Raman design parameters of Gain, Noise Figure (NF) and dispersion in distributed and discrete Raman amplifying devices.*
- *A numerical solution is adapted from the average power to Gaussian pulse sequence at 40 Gb/s bit rate. Integration of the gain and noise profile for signal propagation over a distance of the transmission fiber using the Split-Step Fourier Method (SSFM).*
- *Furthermore the numerical analysis is integrated to a Simulink optical transmission models for transmission performance evaluation of advanced modulation formats such as Amplitude-Shift Keying (ASK) and Multiple-Shift Keying (MSK). Improvement of transmission link distance and noise performance in ultra-long haul transmission are achieved both theoretically and experimentally.*

1 Introductory remarks

Raman scattering phenomenon in glass medium is associated with the molecular diffraction of light, where photons interact with molecules to induce

transitions in energy states. Typically the photons scattered from these interactions are of the same energy and display the same characteristics as the incident light wavelength, known as Rayleigh, or elastic scattering. However a small fraction of light, approximately 1 in 10^7 , is scattered at different optical frequencies and are of a much lower energy level than that of the incident photons, referred as stimulated Raman scattering (SRS) which was in 1928, first discovered by C.V. Raman. The optical effects associated with Raman are of particular importance in the design of currently attracted significant interests in advanced modulation format for lightwave communications systems. The requirements to upgrade existing systems to accommodate for increasing signal transmission quality over longer distances are becoming increasingly important.

In modern long haul fiber-optic communication systems, the transmission distance is limited by fiber loss and dispersion. Traditional methods to overcome this limitation, which use electrical conversion of the optical signal, such as repeaters to retransmit signals at progressive stages are becoming increasingly complex and expensive. In the 1990s, optical amplifiers, which directly amplified the transmission signal, became widespread minimizing system intricacies and cost. While upgrades in transmission fiber design in particular dispersion-compensating fibers (DCF) minimized linear phase distortions in the signal. In modern systems, existing EDFA lumped optical amplifiers are employed to ensure the quality of the transmitted signals. SRS has become important in the application of optical amplification because of several important reasons in comparison to other similar methods. ROA can be described simply as a pump laser which emits lightwaves down an optical fiber; this signifies that it can be compatible with most available transmission systems. The operation of the pump laser is dependant upon the gain that is achieved, in particular the pump wavelength. This means that the medium of transmission is completely independent, in contrast to the lumped optical amplification type, the Erbium-Doped Fiber Amplification (EDFA). The fact that the gain is pump wavelength dependent theoretically means that amplification is achievable for any frequency. It is important to note that utilizing a number of lasers at variable frequencies in a system will provide a broad gain bandwidth. There are also advantages to ROA from EDFA in low noise characteristics, which can improve the overall signal quality [1-15].

This paper summarizes the development of ROA and its application in the transmission of lightwave modulated signals in optical WDM systems. The study is divided into three separate components: (i) The physical model of Raman amplification; (ii) The system transmission model integrating Raman amplification; (iii) Integration of modulation technique minimum-shift keying (MSK) and SRS into the system transmission model.

Stimulated Raman scattering effect has attracted significant commercial interest in its potential technologies for ultra-long haul ultrafast and multi wavelength optical transport engineering. The objectives of this report are to investigate the physical properties of Raman amplification and thence apply them to optical transmission system models that use novel modulation formats, such as ASK or MSK. Comparison of transmission results against different system configurations to determine if ROA is beneficial in expanding span transmission reach and capacity. In particular, it focuses upon the physical modeling of ROA in terms of: (i) Operational principles of ROA, in particular the optical distributed gain and its Noise Figure; (ii) Using MATLAB to numerically solve and analyze these parameters; and (iii) Comparing results of modeling with published documents and other commercially available forms of optical amplification, such as EDFA; (iv) Transposing these results into a SIMULINK transmission models for advanced modulation formats such as ASK, DPSK, MSK etc to achieve improved transmission performance.

2 Lumped and distributed amplifying systems

These roles of distributed and lumped amplification can be illustrated in the schematic diagram of the signal power evolution along the fiber length as shown in Figure 1.

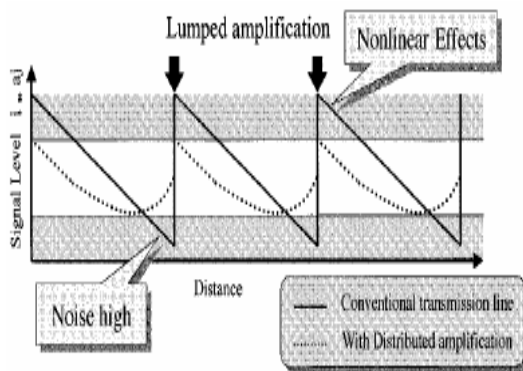


Figure 1 Lumped vs. distributed signal power evolution.

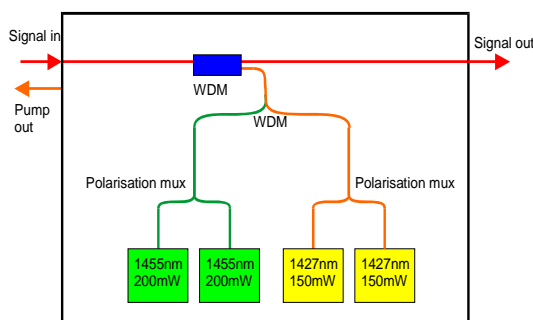


Figure 2: Multiple pump sources arrangement for Raman amplification in DWDM

transmission. Operating band: 1530~1565 nm, Raman pump: multiplexed semiconductor lasers, Pump power up to 500 mW, Gain ripple: 0.8 dB, Small signal gain: 11 dB; OSNR improvement: 4.5 dB; PMD: 0.2 ps, PDG: 0.1 dB

Both forms of optical amplification provide gain to a signal power and are iterated over the fiber spans. However there are some significant differences, both in advantages and disadvantages between these two modes of amplification as follows:

- *In lumped EDFA:* (i) the gain characteristics depend on a large number of device parameters (ii) the signal amplification process starts from the end of the segment and distributed over the effective length as contrasted to the accumulated lumped amplification of the EDFA at the end of a span.
- *In distributed ROA:* (i) the transmission medium, silica fiber, is responsible for the gain characteristics; (ii) gain is delivered backwards from the end of the first lumped circuit and because of the effective length of ROA (in kms) is gradually distributed

Advantages of distributed ROA are that the gain achievable along the transmission fibers, and ease of gain clamping; low noise characteristics; better optical signal-to-noise ratio (OSNR); gain non-resonant and could potentially be obtained for any wavelength; ultra-wide bandwidth gain of about 6THz, wide and flat gain bandwidths achievable using multiple pumps at different wavelengths, increased power budget margins.

Distributed gain is an important aspect in the development of transoceanic high bit-rate WDM transmission. However the disadvantages of the distributed ROA are very high pump powers required; poor pumping efficiency at lower power levels; fast response time which results in higher noises; severe development for existing fiber system; requirement of long gain fiber; severe effects due to nonlinearities.

While for lumped optical amplification, we can identify that: (a) the advantages of Lumped EDFA are the possibilities of integration well into existing systems, due to intrinsic properties of silica, good pumping efficiency at lower powers; widely studied and deployed in WDM systems. (b) the disadvantages of Lumped EDFA are (i) Gain resonant and bandwidth limited to C and L bands (1525-1605nm)(ii) fiber nonlinearities and noise are difficult to resolve ; (iii) difficulty in gain clamping.

It is important to realise while there are some disadvantages to ROA, advancements in fiber technology have been experimented that minimise these issues. A design issue to be considered in this paper is the incorporation of Dispersion Compensation Fiber (DCF) into the system model. The advantages in DCF for ROA

include: (i) High negative dispersion characteristics that could compensate the chromatic and nonlinear dispersion induced in the fiber from GVD and SPM. (ii) Small effective area, hence lower pump power, and high Ge impurity concentration in the silica fiber.

3 Raman Amplification Processes

To appreciate the physical model, it is imperative that the quantum theory of Raman scattering can be explored to gain a broader knowledge of the principal issues. Stimulated Raman Scattering (SRS) is a nonlinear effect due to interactions between light waves with molecular vibrations in silica fiber. It exists when the transmitted power of a channel exceeds the threshold power. For a single lightwave channel we have

$$P_{th} = \frac{16 \cdot A_{eff}}{K_p \cdot L_{eff} \cdot g_r} \quad (1)$$

where K_p is the polarisation constant and assumes a constant 2 for a completely unscrambled signal. The scattering occurs when the polarization of the molecule changes with the vibrational motion. This is caused when an electric field distorts the electrons of the molecule to create an induced dipole moment.

$$\mu = \alpha \cdot E \quad (2)$$

For di-atomic molecule:

$$\alpha = \alpha_0 + \left(\frac{\partial \alpha}{\partial q}\right)_0 q + \dots \quad (3)$$

If the molecule is vibrating with the pump frequency then and there is an oscillating electric field at ν_i frequency:

$$E = E_0 \cos(2\pi\nu_i t) \quad (4)$$

Then the induced dipole moment becomes:

$$\begin{aligned} \mu &= E_0 \cdot \alpha_0 \cos(2\pi\nu_i t) + E_0 \left(\frac{\partial \alpha}{\partial q}\right)_0 A \cos(2\pi\nu_i t) \cos(2\pi\nu_0 t) \\ &\dots = E_0 \cdot \alpha_0 \cos(2\pi\nu_i t) + \frac{1}{2} E_0 A \left(\frac{\partial \alpha}{\partial q}\right)_0 [\cos 2\pi(\nu_i - \nu_0)t + \dots \cos 2\pi(\nu_i + \nu_0)t] \end{aligned} \quad (5)$$

Thus this shows that the moment can oscillate at 3 frequencies and can therefore radiate lightwaves at these optical frequencies corresponding to: Rayleigh scattering (ν_i), Stokes scattering ($\nu_i - \nu_0$) and anti-Stokes scattering (AS) ($\nu_i + \nu_0$).

The emission of light is in the form of energy transitions which will depend on the interaction or collisions between the incident light and the quantum of vibrational energy. Photon energy can be described by as shown in

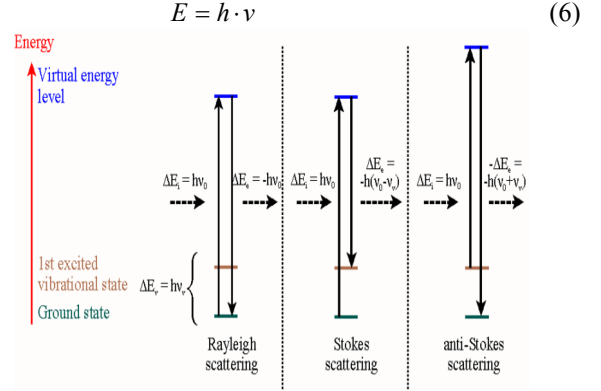


Figure 3: Scattering caused by energy transitions of molecules into excited vibrational states.

In SRS, the scattered photons have energy gained or lost by the incident photons. If the incident photons excite a transition of vibrational energy in the molecule, the scattered photons experience a gain and downshift to the Stokes frequency. In contrast, if vibrational energy already exists in the molecule the incident photon can absorb it, which causes a loss in the scattered photons and up-shifts to the Anti-stokes frequency. The excited vibrational level is populated following a Boltzmann distribution described mathematically as:

$$f(E) = \exp\left(\frac{-E}{k_B T}\right) \quad (7)$$

As anti-stokes scattering is initiated in the excited vibrational level its transition rate is also proportional to this distribution. It is also temperature dependant

$$\begin{aligned} T \rightarrow \infty, I_{AS} &\rightarrow I_S \\ T \rightarrow 0, I_{AS} &\rightarrow 0 \end{aligned} \quad (8)$$

In SRS, because of the relative intensities the Stokes shift is an essential element in the design of Raman amplifiers.

4.1 Raman Amplification Operational Principles

This section investigates the physical model of ROA including the Raman gain, the associated noises in the system and dispersion incurred along the fiber. The frequency difference, $\Omega_R = \nu_i - \nu_0$, the Stokes frequency spectral shift is the essential element in the Raman gain. The intrinsic properties of glass in the transmission medium, usually fused silica, also provides a range that the frequency of the pump, $\nu_p = \nu_i$, and frequency of the signal, $\nu_s = \nu_0$, can differ.

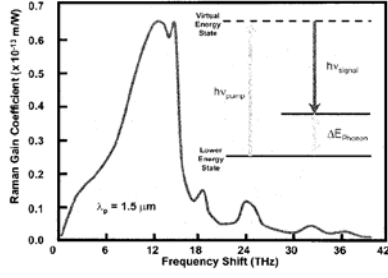


Figure 4: Raman gain spectrum for fused silica [1].

Figure 4 shows the range of up to 20THz that the Stokes shift can vary. The shift which results in maximum Raman gain, g_R at 13.2THz; this corresponds to an approximate wavelength difference of about 100nm between pump and signal. The Raman gain bandwidth $\Delta\nu_g = 6THz$ is defined as the Full-Width Half Maximum (FWHM) of the dominant peak in the gain spectrum. The overall optical gain can be expressed in terms of the pump intensity I_p :

$$g(\nu) = g_R(\nu) \cdot I_p = g_R(\nu) \cdot (P_p / A_{eff}) \quad (9)$$

This equation shows that the gain is dependent upon the frequency and the pump power. The parameter Raman gain efficiency $g_{R,eff} = g_R / A_{eff}$ is a critical design parameter and usually used for the comparison between different fibers that have different gain efficiencies due to smaller effective areas and higher Ge concentrations. That in turn increase the overall Raman gain efficiency, hence the optical gain and lower the threshold power required lasing initialisation and the SRS process.

4.2 Signal and Pump Coupled Equations

The power evolution of the pump (P_p) and signal (P_s) power along the propagation direction of the fiber, z , can be represented by a set of two coupled equations:

$$\begin{aligned} \frac{dP_s}{dz} &= -\alpha_s P_s + \left(\frac{g_R}{A_{eff}}\right) P_p P_s \\ \xi \frac{dP_p}{dz} &= -\alpha_p P_p - \left(\frac{\nu_p}{\nu_s}\right) \left(\frac{g_R}{A_{eff}}\right) P_s P_p \end{aligned} \quad (10)$$

In which the small gain of the signal is g_R , P_p and P_s are the power of the pump and signal beams respectively, ν_p and ν_s are the pump and signal frequency and ξ indicates the polarisation dependency. Eq. (10) illustrates that the pump power provides the energy for amplification and depletes as signal power increases. As pump power approaches the signal power, the optical gain is reduced and gain saturation occurs. In ROA, the laser can be pumped

from either end of the fiber by using different polarisation, $\xi = -1$. The schematic drawing shown in Figure 5 illustrates the bidirectional pumping configuration. Pumping in different directions changes the signal power evolution along the length of the fiber.

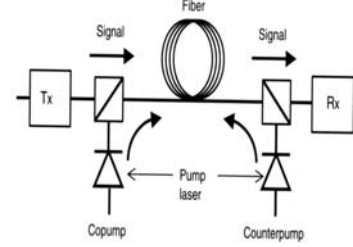


Figure 5: The schematic arrangement of the bidirectional pumping ROA.

The power along the length of the fiber is gradually reduced by the fiber losses. These result in microscopic fluctuations in the density of the core. Doping the fiber with dopants such as germanium further increases these losses. It is also a limiting factor in transmission distance lengths as optical receivers require minimum amounts of power to recover the signal.

This attenuation co-efficient $\alpha_{p,s}$, includes all sources of power attenuation and α is expressed in units of dB/km by the relation $\alpha(\text{dB/km}) = 10 \log(e) \alpha \approx 4.343 \alpha$. If the pump depletion can be neglected, that is in the small-signal amplification regime, the pump-power for forward pumping becomes:

$$P_p(z) = P_0 \exp(-\alpha_p z) \quad (11)$$

with P_0 being the pump-power at the input end. Hence the signal intensity at output of amplifier, length L is determined as:

$$P_s(L) = P_s(0) \exp\left(\frac{g_R P_0 L_{eff}}{A_{eff}} - \alpha_s L\right) \quad (12)$$

The effective length, L_{eff} , is the length over which the nonlinearities still holds or SRS occurs in the fiber and is defined as:

$$L_{eff} = \frac{1 - \exp(-\alpha_p L)}{\alpha_p} \quad (13)$$

As fiber losses also exist at the pump wavelength, it is less than the actual length and can be approximated by $L_{eff} \approx 1/\alpha_p$ if $\alpha_p L \gg 1$. Hence the amplification gain defined as the ratio of the power of the signal with and without Raman amplification, is given by:

$$G_A = \frac{P_S(L)}{P_S(0)\exp(-\alpha_S L)} = \exp(g_o L) \quad (14)$$

This is referred to as the on-off Raman gain and can be determined from Figure 6 from the difference in power of the Raman pumped fiber and the passive fiber without amplification. The difference from the figure is approximately 20dB. Where the small-signal gain, g_o is defined as:

$$G_A = \frac{P_S(L)}{P_S(0)\exp(-\alpha_S L)} = \exp(g_o L) \quad (15)$$

The signal power evolution along the total length of fiber is shown Figure 6 that demonstrates the effect of different pumping configurations.

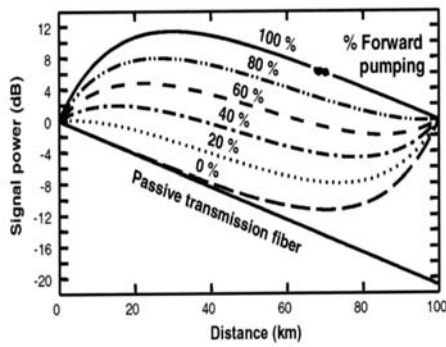


Figure 6: The Theoretical signal evolution using with percentages of forward pumping

4.3 Raman Scattering Noise

In Raman amplification of the signal the noises are contributed by the following processes:

Spontaneous Raman Scattering

In the SRS process noise is added to the amplified signal because of random phases associated with spontaneous generated photons. The spontaneous scattering factor is dependant on the temperature of the amplifier and is defined as:

$$n_{sp} = \frac{1}{1 - \exp\left(\frac{-h\Omega_R}{k_B T}\right)} \quad (16)$$

For a Raman amplifier $n_{sp} \sim 1.13$ as fully inversion of the simulated carrier amplification process always happens. The noise incurred by the spontaneous Raman scattering across the length of the fiber is accumulated and is known as amplified spontaneous emissions (ASE).

Rayleigh Backscattering

Rayleigh backscattering occurs in all fibers and is the fundamental loss in signal power. Typically it

is seen as ASE propagating in the backward direction as is small in comparison to the power of the signal and of no concern. In ROA, however, as a result of large transmission spans it can cause the ASE to be reflected back in the forward direction and re-amplified enhancing the overall noise, this is known as Double Rayleigh Backscattering (DRBS), see Figure 7, and because it can occur anywhere along the fiber it is referred to as Multi-Path Interference (MPI).

Fast response time due to short upper state lifetime

In ROA, the short upper state lifetime results in instantaneous gain which leads to coupling of the pump fluctuations with the signal. To avoid this, backward pumping configurations are adopted which changes the upper state lifetime to the transit time. If forward pumping to be employed, pumps with low noise are required.

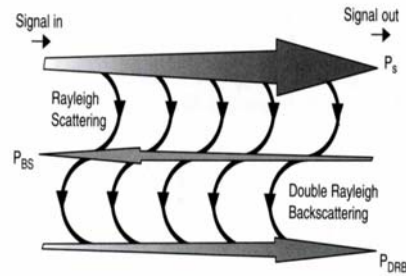


Figure 7: Double Rayleigh Scattering

Noise Figure

The noise figure (NF) is the determination of the signal denigration over the length of the transmission span. It is the signal-to-noise ratio of input over that of the output and in ROA. It is dependent upon the pumping power and the net gain of the system by:

$$NF = 2n_{sp} \frac{g_R}{A_{eff}} \int_0^L \frac{P_p dz}{G(z)} dz + \frac{1}{G_L} \quad (17)$$

where $G(z)$ is the net gain at a distance z along the fiber and G_L is the net gain at the end of the fiber.

4.4 Linear and Non-linear Dispersion

In Raman optical amplifiers, lightwave modulated signals are propagating down a length of fiber which are subject to dispersion due the intrinsic chromatic dispersion properties of a single-mode optical fiber, the wavelength-dependent of refractive indices and the propagation wave number of the fiber profile, of step or graded or multilayer index distribution across the core and cladding regions.

Furthermore nonlinear dispersion, like the non-linear self phase modulation (SPM) effects due to the increased

signal power. In modal description dispersion is related to the group velocities associated with different modes.

Group Velocity Dispersion (GVD)

GVD is caused by chromatic dispersion which exists in fibers that support only the fundamental mode. It causes pulse broadening whereby different spectral components of the pulse are propagating at different velocities and arrive at output of fiber length at different times. The group velocity can be expressed as:

$$v_g = \left(\frac{d\beta}{d\omega}\right)^{-1} s \quad (18)$$

Where β is the propagation constant of the guided fundamental mode along the z-axis. The derivative of the propagation constant in terms of frequency determines the group velocity dispersion (GVD) parameter:

$$\beta_2 = \frac{d^2\beta}{d\omega^2} \quad (19)$$

This parameter determines the pulse broadening effects over the propagating distance. This can be related to the dispersion parameter $D(\lambda)$ as:

$$D(\lambda) = \frac{d}{d\lambda} \left(\frac{1}{v_g}\right) = -\frac{2\pi c}{\lambda^2} \beta_2 \quad (20)$$

As the dispersion can be both negative and positive, it can also be designed at a wavelength of zero dispersion λ_{ZD} around the 1.3 μ m region. It is important that while dispersion is minimised in design, it can not be completely removed as it also minimises the other non-linear effects in the fiber, such the SPM and cross phase modulation (XPM).

Nonlinearity

The SPM causes a nonlinear phase shift (NLPS) in the fiber, the accumulated non-linear phase shift can be solved by:

$$\phi_{NL} = \gamma P_{S0} \int_0^L G(z) dz \quad (21)$$

Where γ the non-linear parameter responsible for SPM is defined as:

$$\gamma = \frac{2\pi n_2}{\lambda_S A_{eff}} \quad (22)$$

Where $n_2 = 2.6 \times 10^{-20} / \text{m}^2$ is the cladding refractive index in fused silica. The NLPS due to ROA, that is the ratio with ROA and without ROA, can be determined by:

$$R_{NL} = \frac{\phi_{NL}(on)}{\phi_{NL}(off)} = \frac{1}{L_{eff}} \int_0^L G(z) dz \quad (23)$$

Pulse broadening can be described by using the wave equation, expressed as:

$$\frac{\partial A}{\partial z} + \frac{j}{2} \beta_2 \frac{\partial^2 A}{\partial t^2} - \frac{1}{6} \beta_3 \frac{\partial^3 A}{\partial t^3} = 0 \quad (24)$$

Where β^3 is the dispersion slope and $A(t,z)$ is a slowly varying amplitude. To incorporate non-linear effects into the pulse broadening equation and compensate for dispersion solitons are integrated in the form of the Schrodinger Equation.

$$\begin{aligned} \frac{\partial A}{\partial z} = & \frac{j}{2} \beta_2 \frac{\partial^2 A}{\partial t^2} + \frac{1}{6} \beta_3 \frac{\partial^3 A}{\partial t^3} + j |A\sqrt{\gamma}|^2 \\ & + \frac{1}{2} [g(\xi) - \alpha] + jTR \frac{\partial |A\sqrt{\gamma}|^2}{\partial t} \end{aligned} \quad (25)$$

This is the un-normalised Non-linear Schrodinger Equation (NLSE) which includes the effects of distributed amplification and dispersion management.

Fibers for distributed Raman amplification

Table 1: Raman gain efficiency of different commercial fibers and the parameters which will be used to numerically solve Raman Amplification.

Type of Fiber	Raman Gain Efficiency (1/Wkm)	Effective Area (um ²)
Allwave	0.35	84.95
Corning NZ-DSF	0.72	80
LEAF (NZ-DSF)	0.45	72
SMF-28 (NDSF)	0.38	84.95
Truewave RS (NDSF)	0.58	60
Truewave Reach Fiber	0.6	55
OFS Raman Fiber	2.5	18.7

Raman Gain efficiency for various fibres

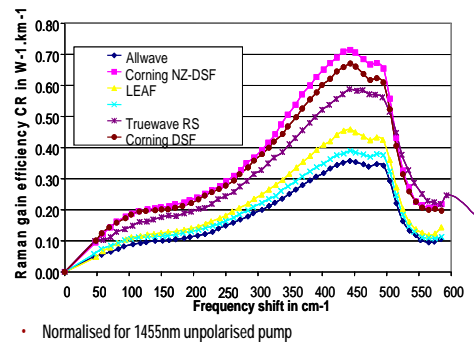


Figure 8 Measured Raman gain efficiency of different installed transmission optical fibers.

Several fibres for transmission can be used as the Raman amplification media. Their scattering coefficients are measured and extracted as shown and interpreted from *Figure 8*. In long-haul transmission it becomes necessary to compensate for dispersion. Dispersion is a linear process whereby pulse spreading can be negated by introducing a fiber with the same degree of GVD but opposite polarization. DCF exist to manage the impact of dispersion with an opposite sign of dispersion and dispersion slope in comparison to SMF. It also has a higher attenuation in comparison to SMF and hence greater noise power.

4 Numerical Modeling of the Coupled Equations

The power evolutions of the pump and signals in a Raman amplified guided medium can be described by a set of ordinary differential equations (ODEs).

$$\begin{aligned} \frac{\partial P_S}{\partial z} &= -(\alpha_{RS} + \alpha_S)P_S + \frac{g_R}{A_{eff}} P_P P_S \\ \frac{\partial N_S}{\partial z} &= (-\alpha_{RS} - \alpha_S + \frac{g_R}{A_{eff}} P_P)N_S + \\ &\dots\dots\dots + \frac{g_R}{A_{eff}} (2P_P N_P)^{1/2} P_S \\ &\dots\dots\dots + (\alpha_{RS} + \alpha_S + \frac{g_R}{A_{eff}} P_P) \frac{h\omega_S}{2} B_0 \end{aligned} \quad (26)$$

$$\begin{aligned} \frac{\partial P_P}{\partial z} &= -(\alpha_{RP} + \alpha_P)P_P \\ &- \frac{\omega_S}{\omega_P} \frac{g_R}{A_{eff}} (P_S + N_S + \frac{h\omega_S}{2} B_0)P_P \\ \frac{\partial N_P}{\partial z} &= -(\alpha_{RP} + \alpha_P)N_P \\ &\dots\dots\dots - (\frac{\omega_S}{\omega_P} \frac{g_R}{A_{eff}} P_S) (2P_P N_P)^{1/2} \\ &\dots\dots\dots + (\alpha_{RP} + \alpha_P) \frac{h\omega_S}{2} B_0 \\ &\dots\dots\dots + (\frac{\omega_S}{\omega_P} \frac{g_R}{A_{eff}} P_S) (2P_P \frac{h\omega_S}{2} B_0)^{1/2} \end{aligned} \quad (27)$$

These equations can be modelled using standard numerical techniques. The particular choice of numerical approximation (e.g. Runge-Kutta etc.) depends upon a specific method (i.e. initial value ODEs), the accuracy required and the consideration of simulation processing time that is especially important under MATLAB and Simulink operating environment. The function ode45.m of MATLAB has been extensively herewith used to solve the coupled equations in which the Dormand-Prince formula meets the required accuracy in the approximation and

in processing time. Assumptions made for the modelling include: (i) Forward and backward noise powers are lower than input signal power by 30dB; (ii) Backscattering powers of pumps and signals are at least 20 to 30dB lower than their original powers. (iii) Noise effects such as spontaneous Raman scattering, Rayleigh backscattering and thermal factor can be reasonably ignored when simulating the Raman gain profile; and (iv) $\alpha_{RS} = \alpha_{RP}$ for simplicity.

The coupled noise equations (26) and (27) have incorporated the fundamental noise sources including zero-point fluctuations, amplification of noise, partition noise and noises due to the Rayleigh scattering.

4.1 Gain

The Raman gain co-efficient is dependant on the difference between the pump and the signal frequencies. In the case where the pump is co-pump with the signal at 1450nm in NZ-DSF, the effects of different shifting frequencies for the signal on the Raman gain are highlighted.

Table 2: Effects of signal frequency shifting on the Effective Raman co-efficient and total Raman Gain.

Shifting Frequency	Signal Frequency	Signal Wavelength	Effective Raman	Raman Gain	
THz	1/c m	nm	1/Wkm	dB	
6	200	200.9	1493.3	0.24	6.61
10.5	350	196.4	1527.5	0.5	13.86
13.2	450	193.7	1548.8	0.72	20.13
16.5	550	190.4	1575.6	0.22	6.06

NZ DSF: Effective Raman Gain vs Shifting Frequency

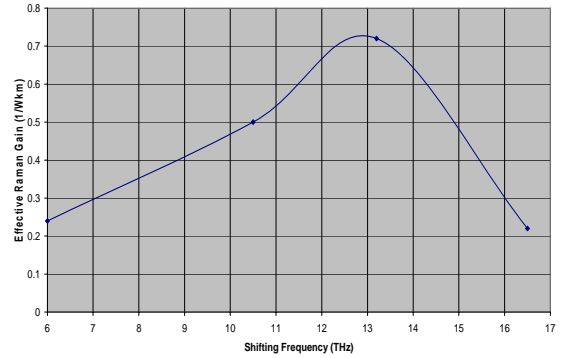


Figure 9 Effective Raman Gain co-efficient versus shifting frequency for NZ-DSF fiber.

Figure 9 demonstrates that the Raman amplification is possible over a wide range of signal frequencies for a single pump, with a peak co-efficient existing at 13.2THz from the pump or approximately 100nm spectral region. Thence, due to the fact that optical amplification is directly proportional to the Raman co-efficient, the optical gain can also be distributed across a wider spectrum.

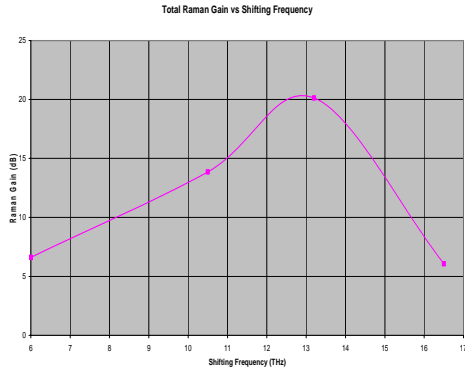


Figure 10: Total Raman gain versus Stoke shift frequency for NZ-DSF.

In a single pumped ROA configuration, we can obtain the high gain and low ripple over the Raman bandwidth as follows. This is possible because individual gain spectra accumulate at the different wavelengths to provide the total system gain over a wide spectral range by combining the pumping wavelengths and pump power using multiple pump sources.

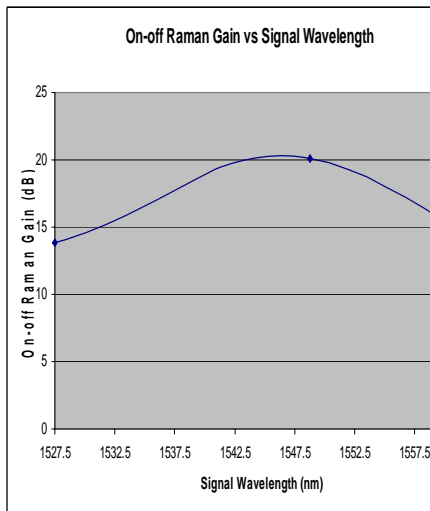


Figure 11: Gain over the Raman bandwidth.

4.2 Distributed Gain

To model ROA in all configurations, forward, backward and bi-directional, two MATLAB ode45 (Appendix B) functions are employed for backward and forward pumping respectively while the signals always propagate in the same direction.

To achieve bi-directional pumping, the effects of the pump power co- and counter-propagating are accumulated to give the total pump power. The pump power is shown to reduce to provide gain for the signal power, this is due to pump depletion. Figure 12

shows the power evolution of the pump along the total length of the Corning NZ-DSF fiber for forward, backward and bi-directional configurations.

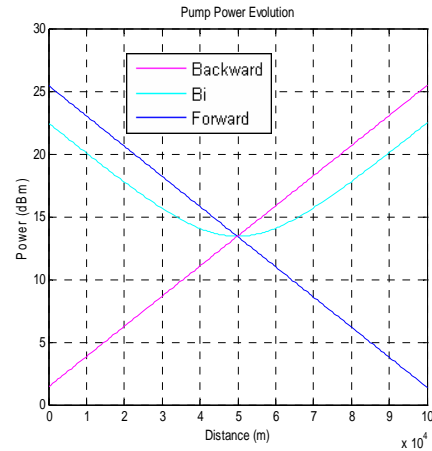


Figure 12: The power evolution of the pump along the total length of the Corning NZ-DSF fiber for forward, backward and bi-directional configurations, blue, magenta and cyan respectively.

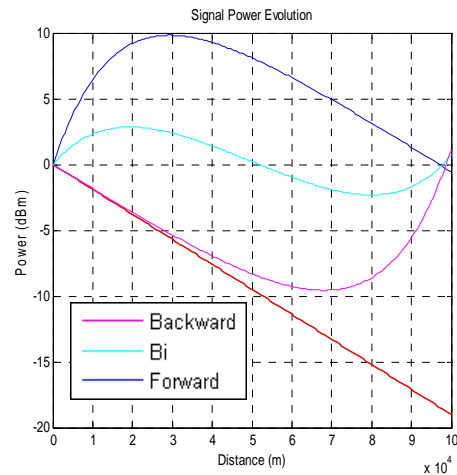


Figure 13: The power evolution of the signal along the total length of the fiber for forward, backward and bi-directional configurations, blue, magenta and cyan respectively. The red line represents a passive fiber with no gain, $\alpha = 0.19\text{dB/km}$.

The signal power evolution shows how it changes the attenuation map in comparison to the passive fiber, with no Raman amplification as illustrated in Figure 13. In the forward configuration, there is a large gain in power at the beginning of the fiber length. This results in increasing effects of non-linearities in the fiber, because of the power dependence of the refractive indices of core

and cladding, approximated by $n^j = n^j + n_2^j(P/A_{eff})$ with $j = 1, 2$. In the backward configuration, the gain occurs towards the end of the fiber after a substantial power loss. This power loss will increase the possibility

of noises altering the quality of the signal. The bi-directional configuration shows a balanced result in terms of noises and non-linearities.

Another important aspect to consider is the on-off Raman gain provided by amplification. In other words the gain experienced with Raman in comparison to gain experienced without Raman. The evolution of gain along the total length of the fiber can be solved through the decibel difference.

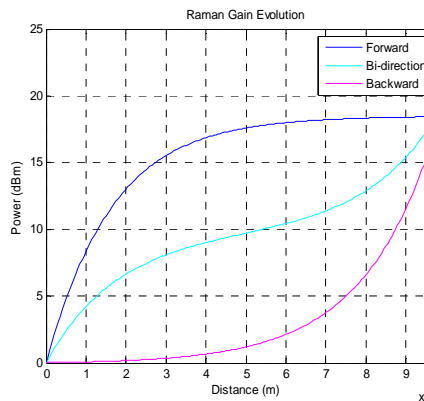


Figure 14: The gain evolution over the total length of the fiber due to Raman amplification for forward, backward and bi-directional configurations.

The on-off Raman gain evolution is an important parameter that needs to be implemented using the split-step Fourier method (SSFM) for Gaussian pulse and ASK transmission Simulink model.

It is also necessary to compensate for the passive fiber losses (Net Gain = 0). This is important because if the signal has a net gain or loss it will be effected detrimentally when it propagates through numerous spans. Table 3 below shows the fibers pumping over a 100km span, typical Raman lasers operate < 500mW, this limits the transmission spans of LEAF, SMF-28 and Allwave.

Table 3: Final Net Gain for different commercial fibers and the required pump power to pump the fiber over the span just compensating fiber losses.

Type of Fiber	Average Power (dBm)			Required PumpPower (net gain =0) ~mW
	For ward	Back ward	Bi-Directional	
Allwave	-9.502	-9.327	-9.397	700
Corning NZ-DSF	0.551	1.128	0.707	350
LEAF (NZ-DSF)	-6.879	-6.529	-6.654	550
SMF-28 (NDSF)	-8.707	-8.491	-8.574	650
zTruewave RS (NDSF)	-3.638	-2.864	-3.099	425
Truewave Reach Fiber	-3.165	-2.297	-2.554	425

To illustrate the numerical simulation evolution, an analytical solution can be derived from the

coupled equations assuming no pump depletion. It is determined that the pump depletion reduces the transfer of power from the pump to the signal as the pump power depletes faster than that of the signal. To further investigate the initial input signal power was increased to approach the initial pump power, it is observed that there is greater reduction in signal gain due to gain saturation. These features are illustrated in Figure 15 and Figure 16.

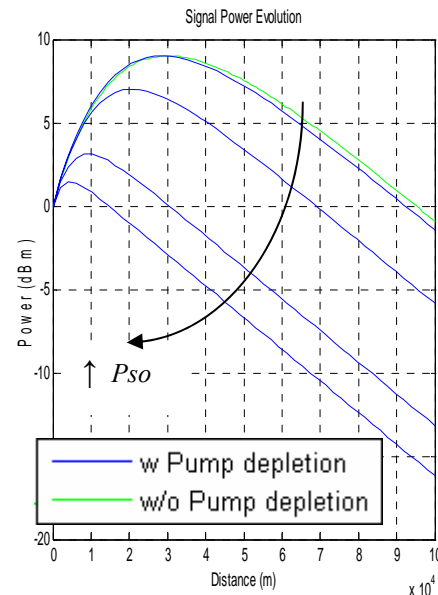


Figure 15: The power evolution of the signal along the total length of the fiber with and without the effects of pump depletion, blue and green respectively.

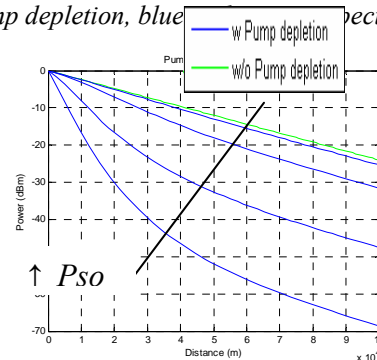


Figure 16: The power evolution of the pump along the total length of the fiber with and without the effects of pump depletion, blue and green respectively.

4.3 Gaussian Pulse Propagation

Numerically solving the coupled equations using the ode45 function in MATLAB can be extensively used to obtain the averaged signal and pump power evolution. To implement into the SIMULINK for ASK-modulation model, this solution must be adapted to Gaussian pulse at the correct bit rate of 40Gb/s. These pulse sequences are propagated numerically using the Split-step Fourier Method (SSFM). The SSFM propagation can be modified to include the Raman amplification. This can be achieved

by changing the SSFM half-step parameter which is the gradient of the attenuation iterated over a number of segments along the fiber. In the passive fiber case the half-step is constant; to include ROA the Raman gain contribution at each point is added to this half-step.

4.4 Noise Figure

Modelling the noise profile, the noise power evolution of the signal along the total length of the fiber can be exploited. The resulting signal noises agree with published results (D. Dahan and G. Eisenstein, 2004). Discrepancies are due to the modelling of the numerical equations modelled included Rayleigh scattering and pertinent noises other than ASE.

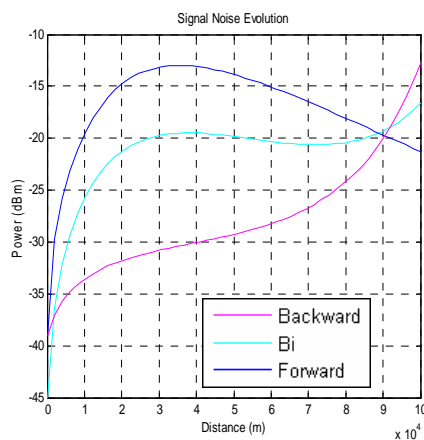


Figure 17: The noise power associated with the signal along the total length of the fiber for forward, backward and bi-directional configurations.

Investigating the signal noise evolution along the fiber is essential so as to estimate the noise figure (NF) of the DRA system. It is a value of the signal denigration over the total span and is proportional to the attenuation and length. Typically for DRA, the transmission link is greater than 50km and the net gain of the signal is below 1. Therefore, from Figure 17, it is shown that the noise figure is typically large for amplification over these lengths.

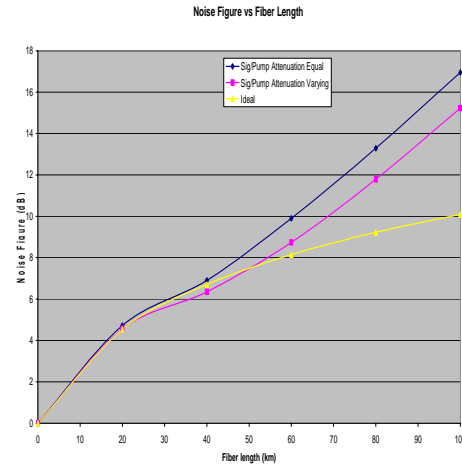


Figure 18: Noise Figure versus on-off Raman gain for backward pumping case and investigating practical and ideal configurations.

Distributed amplification is analogous to numerous discrete amplifiers providing gain along the length of the fiber, ideally, if the loss at each point in the span could be corrected, the ideal noise figure could be determined and expressed as $NF|_{dB} \approx 10 \log(2\alpha + 1)$. For a passive fiber with no DRA (On-Off Gain = 0) over 100km the noise figure degrades by 20dB. By counter-pumping with an On-Off Gain of 20dB the NF is reduced to 17dB. Though there is a high NF it does not mean that distributed amplifiers are noisier than that of the lumped type.

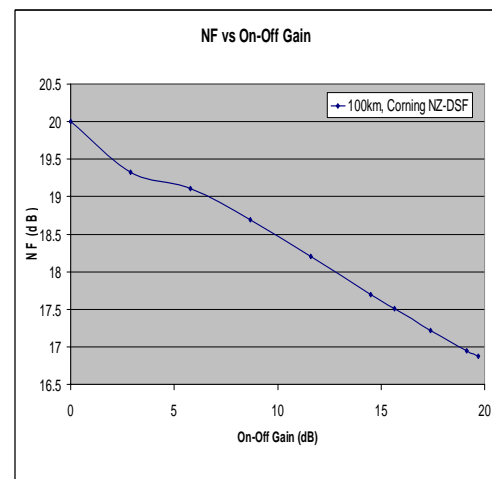


Figure 19: Noise figure versus on-off Raman Gain for a 100km fiber varying input pump power using Corning NZ-DSF.

To evaluate the performance of the DRA in relation to a passive fiber or discrete Raman/EDFA amplifier; it is useful to define the *effective noise figure*: $NF_{eff} = NF_R - \alpha_S L$. It accounts for the attenuation of the fiber and numerically equates the result to an equivalent discrete NF. Therefore, from Figure 20 it can

be observed that the NF_{eff} for backward DRA is equal to -3dB for Corning NZ-DSF. Comparing to a lumped amplifier with a NF limit of at least 3dB the overall improvement of distributed amplifiers is at least 6dB for backward pumping.

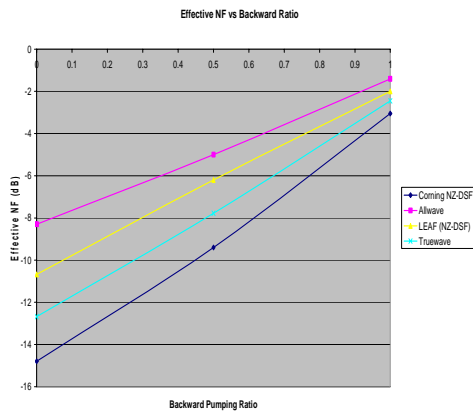


Figure 20: Noise Figure versus backward pumping ratio for different fibers over a 100km transmission link.

The NF is also dependent upon the pumping configuration, as it is dependent upon accumulation of the pumping power and net gain along the fiber. In backward pumping methods the power reduction in signal and therefore net gain is much more dominant and therefore the NF is expected to be much higher. Figure 20 illustrates the impact these configurations have on total NF. It shows an improvement of over 10dB for forward pumping configurations.

When varying the backward pumping ratio for different fibers over the span the different values of NF were determined and showed that for reduced Raman gain co-efficient, g_R , values, the impact of the pumping scheme, forward to backward, on the NF was reduced.

As the NF is dependent upon the pumping power and the net gain, if it is used in a hybrid system configuration, an EDFA pumping gain at the start of the fiber, the NF for ROA can be lowered. These results assume an ideal EDFA, hence $NF = 3dB$ is included in the total noise figure. The NF of the distribute Raman OA and EDFA is tabulated and plotted in Table 4 and Figure 21 respectively.

Table 4: Noise figure of 100km backward-pumped ROA in hybrid configuration with ideal EDFA gain using Corning NZ-DSF.

Ideal Gain (dB)	EDFA/DRA	Noise (dB)	Figure
0		17	
1		19.13	
2		18.27	
3		17.46	

4	16.6
5	15.8
6	15
7	14.09
8	13.25
9	12.45

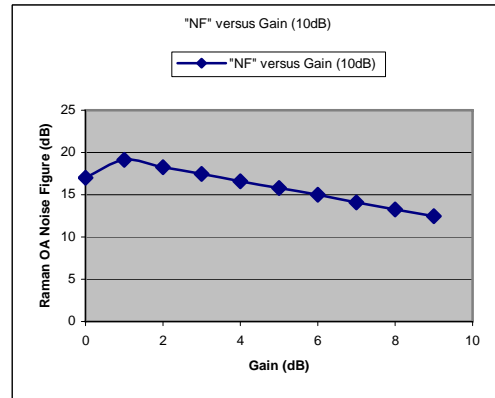


Figure 21 NF of Raman OA versus the optical gain in hybrid AEDFA+ ROA.

4.5 Dispersion

Another important aspect to consider is the effects of dispersion in the fiber. This was tested for all types of system configurations for two fiber of very different fiber properties.

Table 5: Dispersion characteristics for two commercial fibers with different properties in a 100km span [1](Headley, C & Agrawal, 2005)

	Corning NZ-DSF		Allwave		
	NLPS (rad)	Raman NLPS (dB)	NLPS (rad)	Raman (dB)	NLPS
Forward	7.00E-04	13.79	8.00E-04	14.28	
Bi-directional	1.52E-04	7.09	1.53E-04	7.35	
Backward	4.28E-05	1.58	4.14E-05	1.7	

It demonstrates that in the forward pumping scheme, the Raman amplification causes the most non-linear effects due to the increased signal power gained throughout the fiber.

4.6 Discrete Raman Amplification

In the case of lumped Raman amplification the total gain is amplified at the end of the fiber. This gives the saw-tooth effect, for the graph below the discrete amplifier would require a gain of 19dB/km as shown in Figure 22. The convenient aspect of discrete Raman amplification is that its gain profile is dependant upon the coupling equations of distributed ROA. The differing aspect is the fiber properties, referring back to Table 1,

the effective Raman gain co-efficient is much higher and the effective area significantly smaller.

Implementing the discrete Raman fiber properties into the numerical model determines the gain profile as shown in Figure 23.

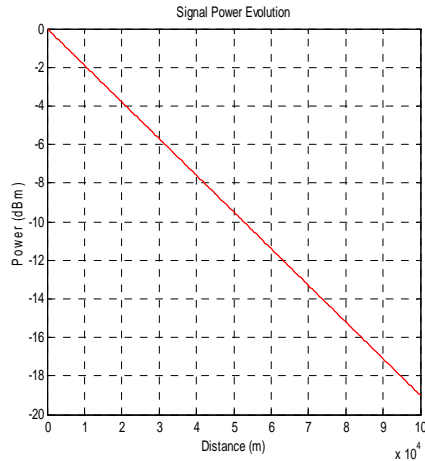


Figure 22: Attenuation map of a passive fiber over the total length without amplification, $\alpha = 0.19\text{dB/km}$.

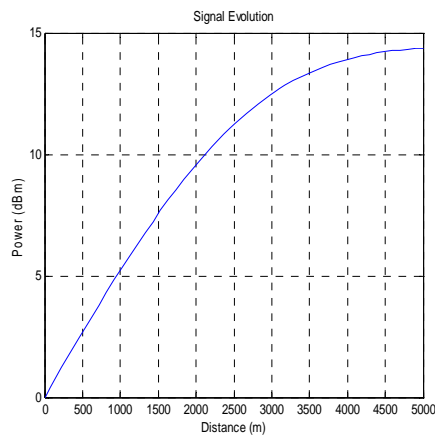


Figure 23: The signal power evolution of a discrete Raman amplifier in the forward configuration.

High net gains are observed over short lengths of fiber, adjusting the pumping power or implementing discrete fibers of differing efficiencies can be used for gain equalisation of the passive fiber loss. Figure 24 shows the signal evolutions for different pumping schemes, these results well agree with the theoretical predictions as reported (Headley, C & Agrawal, 2005); the difference is due to the initial signal channel power and fiber parameters.

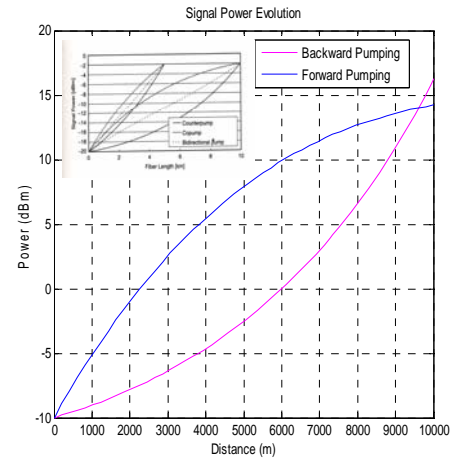


Figure 24: Discrete Raman amplifier signal evolution for forward and backward configurations with $P_{S0}=0.1\text{mW}$ and equivalent theoretical results inserted (Headley, C & Agrawal, 2005)[1]

The noise figures of lumped Raman amplifiers is typically much smaller because of the shorter distances required for the gain to be distributed. For smaller fiber lengths the NF of a discrete Raman amplifier will be at least 3dB because of the thermal excitation of the vibrational modes.

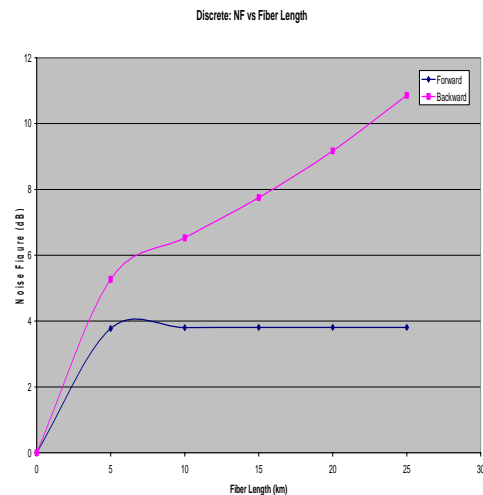


Figure 25: NF versus fiber length for forward and backward pumping discrete Raman amplifiers.

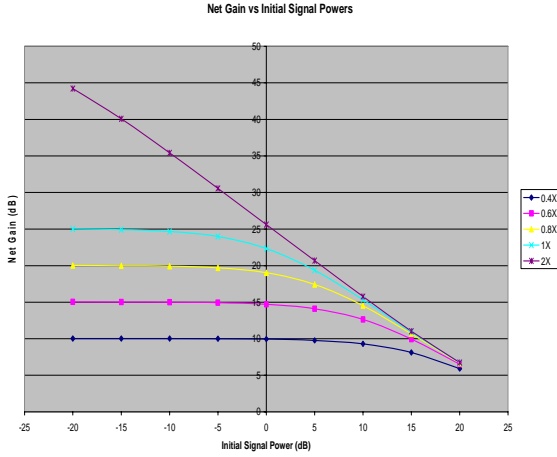


Figure 26: Net Gain versus initial signal powers for different gain efficiencies.

The graph above shows the variation of net gain for different signal powers. The reason that the net gain increases for different Raman gain efficiencies is because the larger efficiencies make output $P_S \rightarrow P_P$ and hence cause more gain saturation.

5 Non-Linear Raman Gain/Scattering Schrödinger Equation

This section illustrates the Raman gain model for SSMF and DCF. The models revolve around the Non-linear Schrödinger's (NLS) equation, as it governs propagation of optical pulses inside fibers. Thus if any distributed amplification is to take place, this equation must be transformed to incorporate Raman amplification. The NLSE as solved for the ASK model before manipulation is:

$$\frac{\partial A}{\partial z} = -\frac{j}{2}\beta_2 \frac{\partial^2 A}{\partial t^2} + \frac{1}{6}\beta_3 \frac{\partial^3 A}{\partial t^3} - \frac{\alpha}{2}A + j\gamma \left(|A|^2 A + \frac{i}{\omega_0} \frac{\partial}{\partial T} (|A|^2 A) - T_R A \frac{\partial |A|^2}{\partial T} \right) \quad (28)$$

The NLSE incorporates fiber losses through the use of the attenuation factor α and second and third-order dispersion (TOD) effects through the use of β_2 and β_3 respectively. T_R becomes negligible as it is almost insignificant. The Non-linear Schrödinger's equation that incorporates distributed amplification and dispersion management is:

$$\frac{\partial u}{\partial \xi} = \frac{j}{2}\frac{\partial^2 u}{\partial \tau^2} + \delta \frac{\partial^3 u}{\partial \tau^3} + j|u|^2 u + \frac{L_D}{2} [g(\xi) - \alpha] u - j\tau_R \frac{\partial |u|^2}{\partial \tau}$$

(29)

The first Schrödinger equation (11) is un-normalised, meaning that it can be subjected to modelling techniques as it is represented in its raw entirety. The second equation (12) is normalised, meaning that it has been transformed into its un-normalised state. The overall resultant equation can be shown as

$$\frac{\partial A}{\partial z} = \frac{j}{2}\beta_2 \frac{\partial^2 A}{\partial t^2} + \frac{1}{6}\beta_3 \frac{\partial^3 A}{\partial t^3} + j|A\sqrt{\gamma}|^2 + \frac{1}{2}[g(\xi) - \alpha] + jTR \frac{\partial |A\sqrt{\gamma}|^2}{\partial t} \quad (30)$$

where: $\gamma = \frac{2\pi n_2}{\lambda A_{eff}}$; $\xi = \frac{z}{L_D}$ and $L_D = \frac{T_0^2}{|\beta_2|}$. T_R term can be

negligible, resulting in the equations shown earlier. β_{1z} term is a purely delay term and can be removed without affecting the pulse envelope evolution. It must also be noted that the $g(\xi)$ term can be solved for the three cases of forward, bi-directional, and backward pumping.

5.1 Fiber Nonlinearities

Fiber nonlinearities are very important when considering Raman amplification within transmission fiber. The refractive index of germanosilicate fibers changes with the intensity of the light propagating through the fiber. The nonlinear propagation effects relevant to the evolution of the electric field amplitude involve a cubic term in the electric field, which can be seen in the NLS equation. In a communication system with multiple signal channels, the nonlinear effects are typically classified by the number of field amplitudes involved in the process, each associated with its own frequency. Three fiber nonlinearities that are caused due to the power dependency upon refractive index are: the Self Phase Modulation (SPM), the Cross Phase Modulation (XPM) – and the Four Wave Mixing (FWM). Other types of nonlinearities are the two major scattering effects that take place due to the intrinsic properties of optic fiber are Stimulated Brillouin Scattering (SBS) and Stimulated Raman Scattering (SRS). Both scattering effects shift the frequency of the signal downwards. These effects are considerably more dominant at high pump powers as the intensity of scattered light grows exponentially once a power threshold is exceeded. Throughout this thesis SRS has been the theoretical foundation behind the amplification process and requires a large pump power to be produced. This is the reason why such high pump powers are required when

implementing Raman amplification techniques. SRS does not contribute to fiber losses like SBS does. Input powers less than 10mW are low enough for SRS to not take place, whereas SBS does not need high pump powers to provide loss to the signal.

5.1 Dispersion

From the start of its invention, optic fiber has been taken advantage of and has been stretched to reach its limits. The realisation of the limits of optic fiber were not realised until its full implementation and greater transmission rates were passed through. Dispersion is a term that has been rarely mentioned in this document, but is of great importance in transmission systems. Dispersion can be classified as two separate effects, chromatic and polarization mode.

Chromatic dispersion represents the fact that different colours or wavelengths travel at different speeds, even within the same mode. Chromatic dispersion is the result of material dispersion, waveguide dispersion, or profile dispersion. Polarization mode dispersion (PMD) is another complex optical effect that can occur in single-mode optical fibers. Single-mode fibers support two perpendicular polarizations of the original transmitted signal. If it were perfectly round and free from all stresses, both polarization modes would propagate at exactly the same speed, resulting in zero PMD. However, practical fibers are not perfect; thus, the two perpendicular polarizations may travel at different speeds and, consequently, arrive at the end of the fiber at different times [10]. Generally the effects of PMD are smaller than any given data rate, thus it will be ignored for the sake of this thesis.

5.3 Split-Step Fourier Method

The numerical method used to solve the nonlinear Schrödinger equation is known as the Split-Step Fourier Method (SSFM). It accurately models the fiber nonlinearities within the system. This method only applies to the un-normalised expression of the Schrödinger equation and requires the NLS equation to be transformed into:

$$\frac{dA}{dz} = A(\hat{D} + \hat{N}) \quad (31)$$

where \hat{D} represents the differential operator that accounts for dispersion and absorption in a linear medium, and \hat{N} is a nonlinear operator that governs the effect of fiber nonlinearities. The resulting un-normalised NLS equation in split-step form can be represented as:

$$\begin{aligned} \hat{D} &= \frac{j}{2} \frac{\partial^2 |\beta_2|}{\partial t} + \frac{1}{6} \frac{\partial^3 \beta_3}{\partial t} + \frac{1}{2} [g(\xi) - \alpha] \\ \hat{N} &= j |A\sqrt{\gamma}|^2 + jTR \frac{\partial |A\sqrt{\gamma}|^2}{\partial t} \end{aligned} \quad (32)$$

The nonlinear effects and dispersion work in conjunction within transmission fiber. As SSFM is only an approximation method, these two factors can be broken up and solved individually. The Schematic illustration of the symmetry split-step Fourier method used for numerical simulations is shown below.

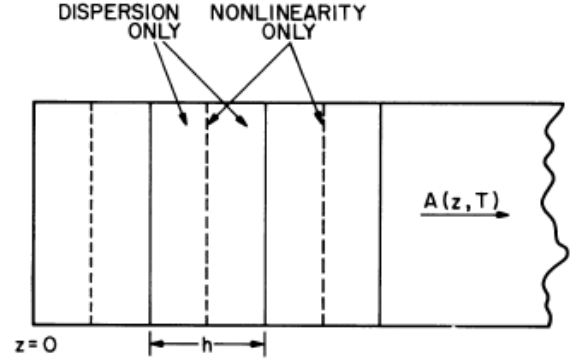


Figure 27: The Span in Closer View by the SSFM [G.P. Agrawal, 'Nonlinear Fiber Optics'] [3]

The fiber length can be divided into a large number of micro-segments of step length h . Within a segment, the effect of nonlinearity is included at the mid-plane shown by a dashed line. Both dispersion and nonlinearity can be solved through an analytical approach which involves converting from time domain to Fourier domain then inverse Fourier domain and then back into time domain.

6. Raman Optically Amplified Gaussian Pulses and Transmission Performance

The Split-Step Fourier Method (SSFM) under the influence of Raman amplification can be modelled and tested using Simulink. Testing the propagation can be under a theoretical Gaussian pulse through the fiber and check whether the Gaussian pulse that is theoretically transmitted is coming back out with either a gain or loss, depending on initialisation parameters. The resultant Gaussian pulses from the propagation program are compared to the eye diagrams from the ASK model, which are both in turn compared to that of the numerical solution. This numerical solution had to be added to give gain to both the system and propagation models.

An eye diagram can be used to estimate the Bit Error Rate (BER) of the System. Once the value of S/N is found then the BER can be determined using:

$$BER = \frac{1}{4} \left[\operatorname{erfc} \left(\frac{I_1 - I_D}{\sigma_1 \sqrt{2}} \right) + \operatorname{erfc} \left(\frac{I_D - I_0}{\sigma_0 \sqrt{2}} \right) \right] \quad (33)$$

where $Q \equiv \frac{(I_1 - I_0)}{\sigma_1 + \sigma_0}$; and σ is the standard deviation from the mean, μ which equates to approximately 34.1% of the information.

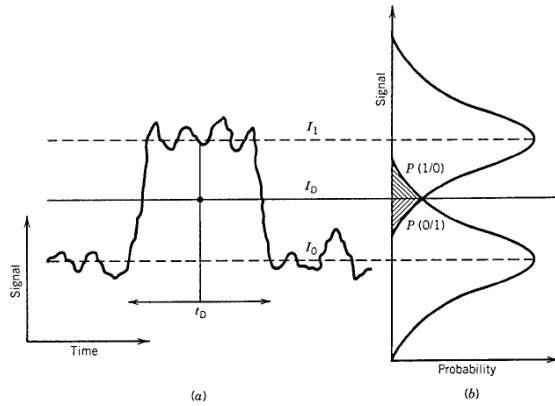


Figure 28: (a) *Fluctuating Signal at Receiver and (b) Gaussian probability density*

This section focuses on the modelling techniques for the lightwave modulated signals travelling through the fiber. The NLSE is derived and the propagation equation over a single-mode optical fiber is given. Shown in Table 6 is a table depicting the typical optical fibers commonly installed throughout the global networks and the required pump powers to make the signal reach back to net gain zero for a length of 100km of fiber.

Type of Fiber	Raman Gain Efficiency γ (Geff)	Effective Area (μm^2)	Required Pump Power for Net Gain = 0 (mW)
Allwave	0.35	84.95	700
Corning NZ-DSF	0.72	80	350
LEAF (NZ-DSF)	0.45	72	550
SMF-28 (NDSF)	0.38	84.95	650
Truewave RS (NDSF)	0.58	60	425
Truewave Reach Fiber	0.6	55	425

Table 6: *Fiber Properties*

Table 6 provides the required pump power decreases when the Raman gain coefficient is increased. The ideal fiber for the modelling application is the Corning NZ-DSF. These parameters can be confirmed by our numerically solved the coupled equations that govern Raman amplification as described above. This program is then incorporated into the Gaussian propagating program and then the ASK modulation format transmission model. For Corning fiber the dispersion can be estimated as¹:

$$D_\lambda = \frac{S_0}{4} \left(\lambda - \frac{\lambda_0^4}{\lambda^3} \right) \quad (34)$$

where $S_0 = 0.093 \text{ ps}/(\text{nm}^2 \cdot \text{km})$, $\lambda_0 = 1302\text{-}1322 \text{ nm}$, $\lambda = 1550\text{nm}$ (operating wavelength). Thus the dispersion calculated is approximately equal to $17 \text{ ps}/(\text{nm} \cdot \text{km})$.

The simulation program output gain profiles obtained in previous sections could then be transferred into the propagation program to help add gain to the NLSE which in turn underwent the Split-Step Fourier Method. Below are some of the results achieved by the numerical solution of the coupled equations.

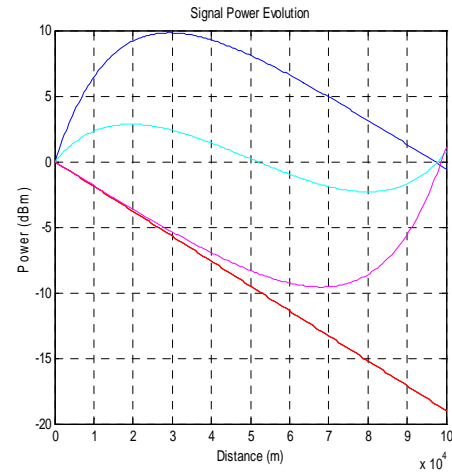
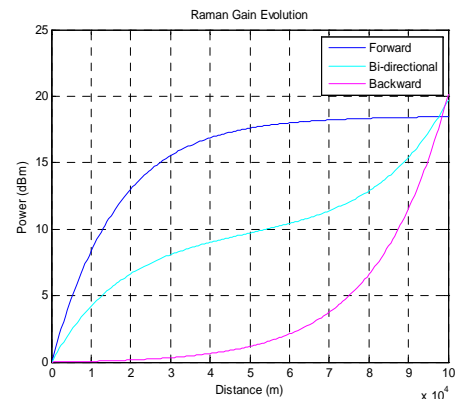


Figure 29 *The power evolution of the signal along the total length of the fiber.*

In the simulation of the Raman gain obtained in Figure 29 the following values are assumed $\alpha_s = 0.19 \text{ dB/km}$, $\alpha_p = 0.24 \text{ dB/km}$, Effective Area ($A_{\text{eff}} = 80 \mu\text{m}^2$, Raman Gain Co-efficient = $0.72 \text{ W}^{-1} \text{ km}^{-1}$. The plot above depicts the power over the length of the fiber. Forward (blue), Backward (magenta), Bi-Directional (cyan) pumping techniques are shown, along with passive fiber (red). The typical net gain at the end of the fiber is approximately zero.



¹ Corning Inc. NZDSF Fiber Characteristics

Figure 30: *The gain evolution over the total length of the fiber due to Raman amplification.* Bi-Directional Pumping Case

Figure 30 shows the gain profile over the length of the fiber, which is of great importance as this is the result that must be implemented into the propagation program which uses SSFM to simulate the transmission of signal over fiber. As the attenuation due to the signal is constant over the fiber, it can be considered a constant gradient. To incorporate the gain into the NLS equation, it too had to be converted into gradients, so it could be simply added to the attenuation map.

Once the NLSE incorporates the Raman gain and is solved using the SSFM propagation program. The Split-Step Fourier Method is tested with a single Gaussian pulse.

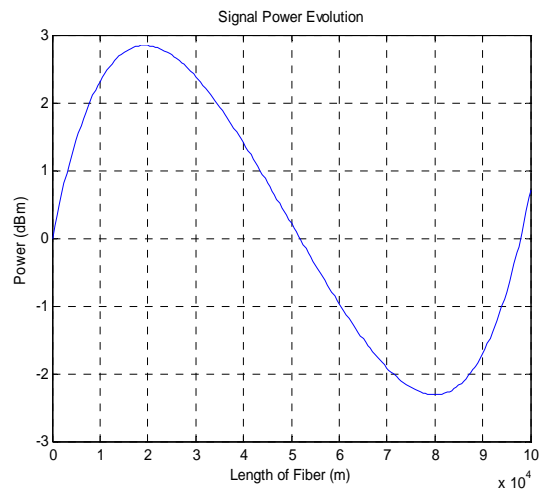


Figure 32: *Signal Power Evolution: Bi-Directional Pumping*

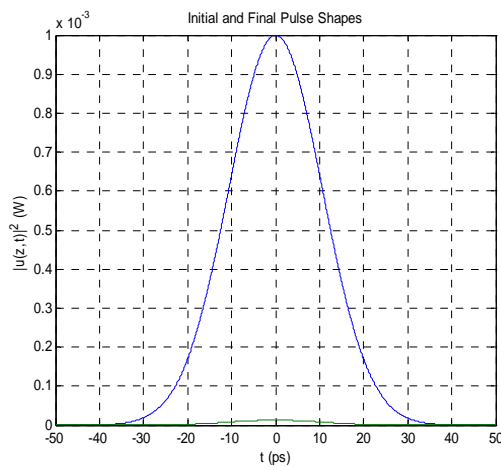


Figure 31: *Gaussian Pulse Before and After Transmission*

In all the Gaussian pulse propagation cases presented throughout this section, the input pulse is depicted in blue and the output in green. In this first case the input pulse was 1 mW and the output 0.01258 mW. The power lost over 100km of SMF fiber is -19.0032. The next type of testing with the Gaussian pulse inputs of the three configurations of Raman amplification media. The lengths are left the same and the pump power maximum used is 350 mW in either forward or backward cases, or 175 mW at both ends under bi-directional pumping.

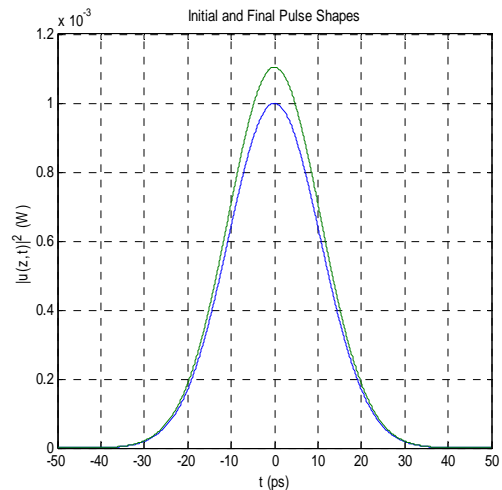


Figure 33: *Gaussian: Bi-Directional Pumping*

Figure 32 shows the Signal Power Evolution over the length of the fiber. As observed the fiber experiences backward and forward power gains, due to the power from pumps being implemented in the forward and backward direction, hence the term bi-directional. At the end of the fiber the expected output is 0.7075 dB. To check to see whether the output obtained from the split-step method is correct, one must look at the output Gaussian pulse. The peak at the output is 1.104 mW, i.e. $10\log(1.104/1) = 0.4297$ dB. The expected output is 0.7075 dB, thus there is a small discrepancy between the two functions.

Forward Pumping Case

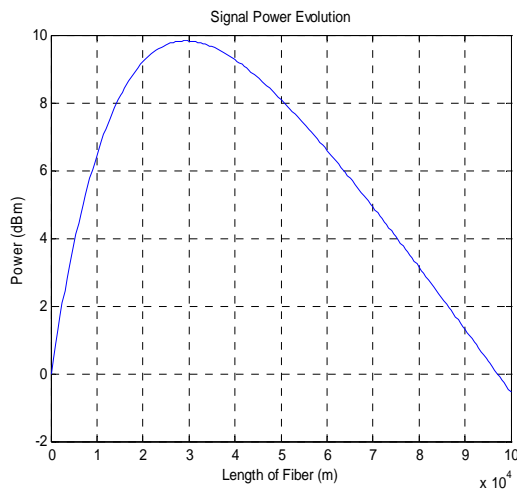


Figure 34: Signal Power Evolution: Forward Pumping

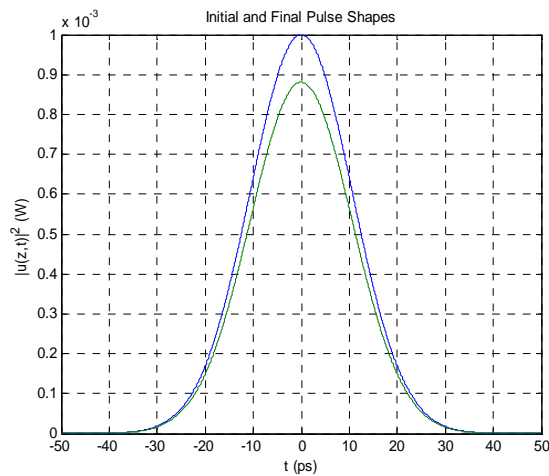


Figure 35: Gaussian: Forward Pumping

Figure 34 shows the evolution of the signal output from the end of the fiber which is -0.5503 dB after undergoing a forward gain. The output as seen by the graph above is 0.8803 mW. This in turn correlates to a gain of $10\log(0.8803/1) = -0.5537$ dB. That means the forward case is almost identical to the numerical model result of -0.5503 dB.

Backward Pumping Case

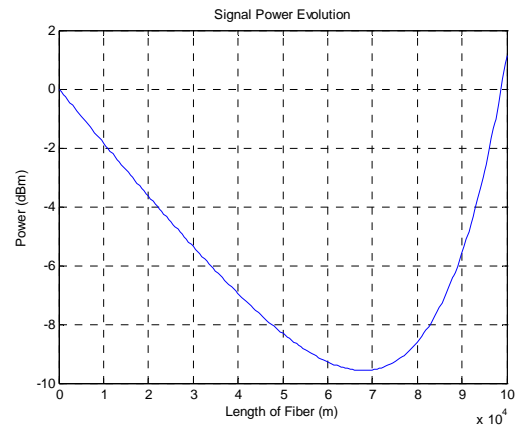


Figure 36: Evolution of the Signal Power under Backward Pumping

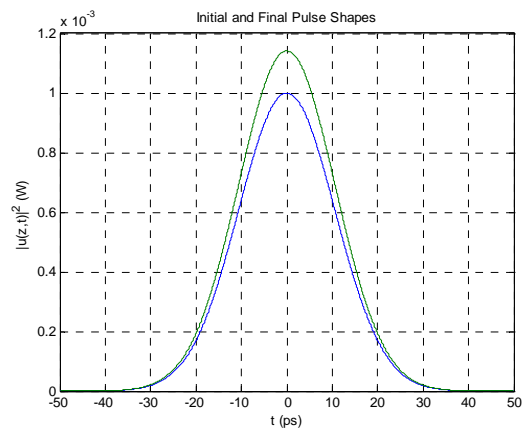


Figure 37: Gaussian pulses under Forward Pumping

The output of the signal obtained from the end of the fiber is 1.128 dB after undergoing backward gain whereas a final pulse of 1.141 mW on the Gaussian correlates to $10\log(0.8803/1) = 0.5729$ dB. As observed, there are inaccuracies in the three pumping techniques presented. This is due to a number of factors including the numerical approximation of the gain curves, the gradients used from the gain curves and the implementation of the Fast Fourier Transform (FFT) for solving the NLSE.

6.ASK optical system transmission

Back to back performance

The initial characteristics of the ASK model need to be tested before simulation can take place. The first eye diagram is an illustration of the input from the system. There is no fiber between transmitter and receiver.

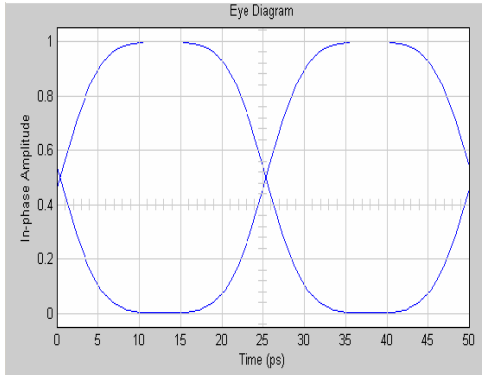


Figure 38: *Input Signal from the ASK Transmitter*

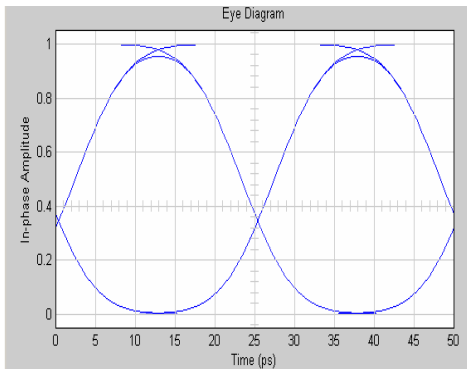


Figure 39: *Output Signal at the ASK Receiver*

The output eye-diagram is as expected even though the output is diluted, the eye is clearly distinguishable, and thus what is transmitted is being received. Note that the pulse width is as initialized, 25 picoseconds.

Transmission fiber but no amplification (Passive Fiber)

The following plots represent the ASK model working over fiber, but no amplification is taking place. The first plot represents the Gaussian output over 3km of fiber with $P_0 = 1\text{mW}$ and a total Length of Fiber = 3km.

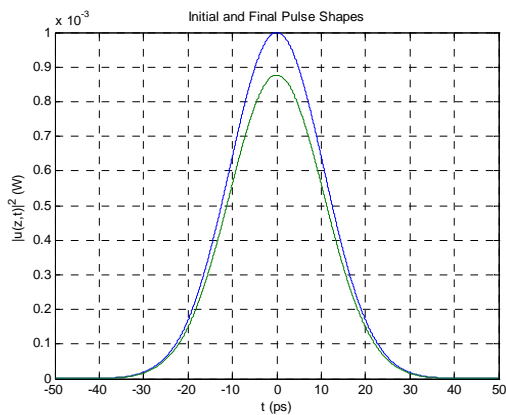


Figure 40: *Gaussian: 3km Passive Fiber*

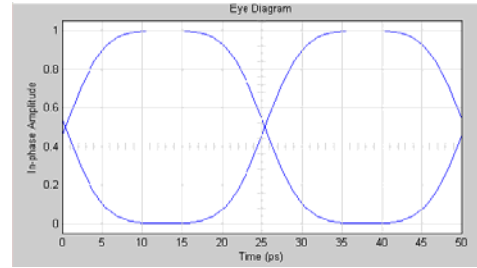


Figure 41: *Input Signal from the ASK Transmitter (Passive Fiber)*

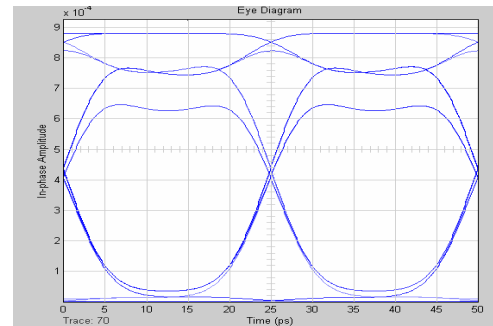


Figure 42: *Output Signal at the ASK Receiver (Passive Fiber)*

As can be seen from above, both the eye-diagram at the output stage and the Gaussian pulse correlate. At the output stages, both diagrams show amplitudes of approximately 0.88 mW correlating to a loss of 0.5552 dB. Theoretical foundation depicts the loss at 0.57 dB, leaving only a small permissible error.

ASK with fiber Amplification random pulse sequence as compared to Gaussian single pulse

Forward Pump Power = 0.4W and Backward Pump Power = 0 W

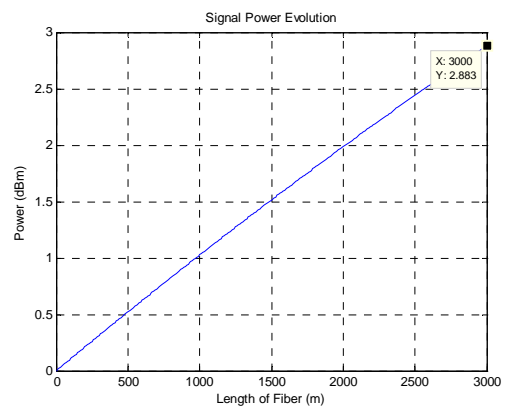


Figure 43: *Signal Power Evolution: Forward Pumping*

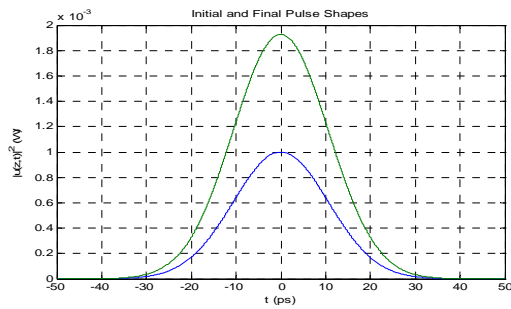


Figure 44: Gaussian: 3km Forward Pumped Fiber

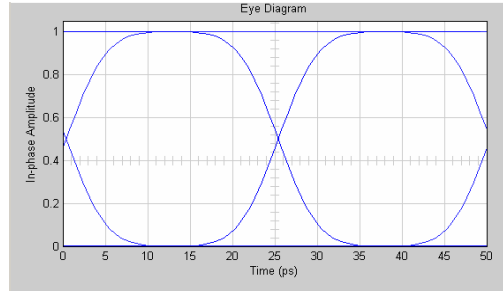


Figure 46: Input Signal at the ASK Transmitter (EDFA Forward Pumped Fiber)

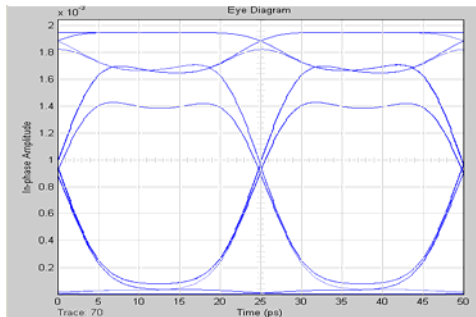


Figure 45: Output Signal at the ASK Receiver (Forward Pumped)

As can be seen from Figure 45, the expected output is 2.883 dB. On the Gaussian plot the output obtained is $10\log(1.928) = 2.8511$ which also matches that of the output eye-diagram. The output shows that the amplitude of the eye diagram is correlating with that of the Gaussian pulse. This is of no surprise as the signal runs through the same process as the Gaussian pulse. As indicated earlier, the noise experienced in the ASK model is due to the numerical approximation of the gain curves, the gradient functions used from the gain curves and the implementation of the Fast Fourier Transform (FFT) used to solve the NLS equation and therefore cannot be solved, only minimized when using this estimation technique.

Transmission span integrated with EDFA Over 99km SSMF +DCF (1km Mismatch)

The following results were obtained after running the ASK model that was originally given to the group. As it was, it contained 50km SMF fiber, an EDFA, 49 km DCF and then another EDFA. Below is the eye diagram for the input. The reason that there is a mismatch between the fibers is due to the system requiring dispersion to reduce nonlinear effects within the fiber.

The pulse width is 25 ps, which is the expected result after the initialization file is run. This corresponds to a 40 Gb/sec transmission rate.

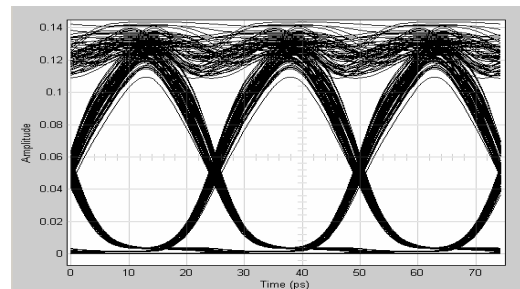


Figure 47: Output Signal of ASK Model (20dB gain EDFA only)

The input power into this system is 1mW, thus there is quite a large gain as the output is approximately 0.13 W which equates to an overall system gain of $10\log(0.13/0.001) = 21.1394$ dB. This is quite unrealistic, and exceeds the power needed at the receiving end, thus the overall system gain should be dropped back down to approximately zero. There is two ways of achieving this, increasing the length of the fiber or decreasing the amount of gain that the amplifiers provide. As there needs to be a comparison between the ASK model with EDFAs and Distributed Raman Amplification, the length was kept consistent, and the EDFA gains were changed from 20 dB to 9.5dB and noise kept at the same ratio, thus decreasing it to 2.375 dB. The eye diagram on the next page was achieved, showing a signal peak of approximately 1mW. This is more realistic, as the input signal is the same as the received signal and falls within a reasonable operating range. It must also be noted that the signal becomes a lot less noisy, due to the fact that the EDFA is not providing too much gain, which in turn provides greater noise in the system.

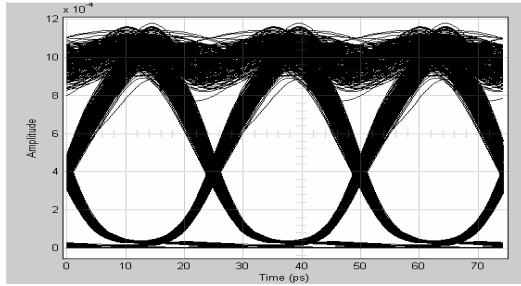


Figure 48: Output Signal of ASK Model (9.5dB gain EDFA only)

Distributed Raman Amplification 1 km SMF mismatched 100 km span

The following figure depicts the output of the ASK model when using Distributed Raman Amplification (Input is the same as that of the previous model).

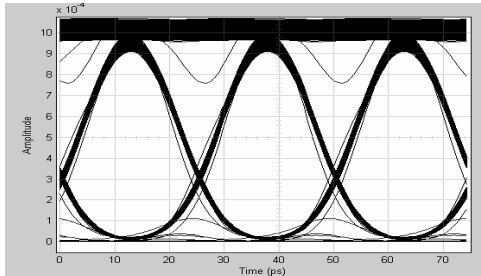


Figure 49: Output Signal of ASK Model (DRA model).

The output peak power of this particular model correlates to that of the input. The accuracy of the result could be made a lot clearer than what is presented. But, as mentioned before, the use of the Fast Fourier Transform (FFT) degrades the accuracy of the algorithm taking place, the Split-Step Fourier Method (SSFM). It must be noted that the Raman amplification model implemented in this section did not account for any noises that could have been added to the transmission signal.

Bit Error Rates

When taking bit error rates into account, the noise of Raman amplification must be added. To check the differences in BER between Raman models with/without noise, both of them have been included with the EDFA model. This process gives an estimated description as to what the effects of noise are on the transmitted signal. The bit error rates for the three systems have been calculated using the equations as given by Agrawal² and as mentioned earlier. To make the process of calculation easier, these equations were made into a Matlab program, which can be seen in the appendices. The table below

² GP AGrawal, "Fiber Optic Systems", 2 Ed., Academic Press 2002.

shows the Bit Error Rates (BERs) for the two systems and the effect that mismatching has upon the system.

k m	BER			Q Parameter		
	EDFA	Raman no Noise	Raman with Noise	EDFA	Raman no Noise	Raman with Noise
0	1.33E-77	8.03E-268	4.34E-117	23.8123	47.4096	31.9322
1	4.76E-62	7.01E-164	3.04E-94	22.9173	33.6381	26.9262
2	2.05E-54	1.21E-144	1.22E-71	19.1478	28.6273	20.9189
3	1.04E-41	5.77E-83	2.79E-49	14.174	23.3518	16.129
4	9.41E-17	3.90E-22	3.49E-19	11.3113	11.5046	11.7835
5	9.85E-15	4.90E-13	4.93E-13	8.939	7.5701	7.4943

Table 7: Bit Error Rate and Q Factor for Different Mismatching.

The table above illustrates the differences between the three models' error rates after undergoing changes in mismatching. All three amplification techniques have low BERs when the mismatch is zero, then starts to increase as the mismatch increases. This correlates in accordance with theoretical foundations, As the Q parameter increases, the BER improves, thus Q is inversely proportional to BER.

Hybrid EDFA-ROA transmission

Hybrid testing of the transmission system involved the addition of Raman amplification and EDFAs to coexist in a single system model. The EDFA is implemented after both the SMF and DCF fibers. The length of the fiber is increased to 100 km (span = 200km) and the pump power is decreased to 100mW in the backward direction, therefore the gain required by the EDFAs is 13.26dB. This is found out by first testing the Raman amplification in the Gaussian program and then deducing the amount of gain required to boost the signal back to a net gain of zero. Below is the eye diagram obtained at the end of a single span for a hybrid structure of distributed and lumped amplification devices. No dispersion mismatch between the two fibers is set.

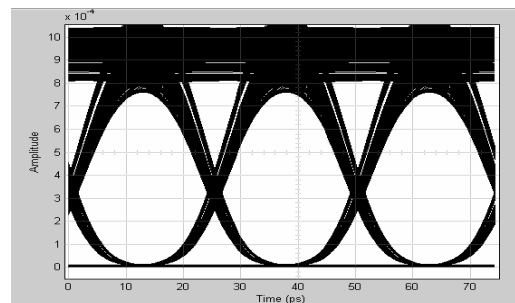


Figure 50: Output Signal of ASK Model (Hybrid model).

The resultant Q parameter and BER are 10.8830 and 4.8712e-013 respectively. This is noticeably higher than that of the Raman and EDFA models when they were in the same position. This could be due to a number of reasons like the amount of noise being added to the

system is considerably higher due to both amplification techniques working in tandem. Thus, from the results obtained it would be safe to say that Raman amplification only is a good model for use in transmission.

It must be noted that this model had lengthy spans of 100km, which in turn should not be compared to that of the previous section. When the length of the fibers were decreased to 50 km each (span=100km), the total BER and Q parameter were $4.8712e-013$ and 9.8450 respectively.

Multi-span transmission

The final set of testing was to find out the typical distance at which Raman amplification can take the transmission signal without regeneration. It was found to be approximately 2000 km. The testing involved only one signal being sent down the fiber, due to the slow operating times of the ASK model under typical operating techniques. Also the effective noise of the signal was not added, as it was only a rough estimate. When implemented, the length before regeneration was required when noise was implemented into the system was found to be 800km. This is a considerable drop compared to that of the amplification model without noise.

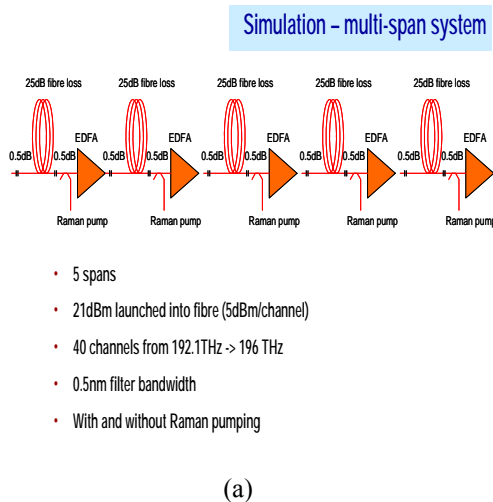
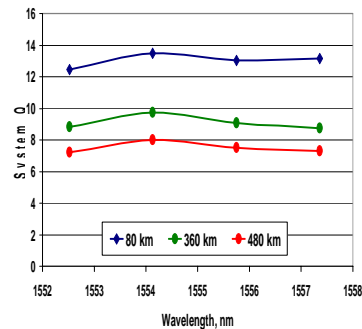


Figure 51 System simulation arrangement of a 4-span DWDM hybrid EDFA/ROA transmission 40Gb/s CS-RZ transmission system of 120 km /span.

Extended Span NDSF Systems without Raman



• Span extension $Q > 7$ demonstrated for 480 km system at 120 km span length

480 km extended span NDSF system with one distributed Raman amplifier

• Q improvement by 0.8 unit with Raman pre-amplification
• Margin available for further extension of span length

Figure 52 Transmission span expansion 4-span 40Gb/s CS-RZ transmission system of 120 km /span (a) without Raman OA (b) with one Raman OA in one span.

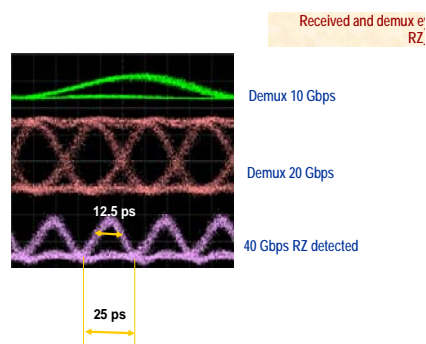


Figure 53 Received eye diagrams of the transmission of random bit pattern over transmission span expansion 4-span 40Gb/s CS-RZ transmission system of 120 km /span with one Raman OA in one span.

Experimental demonstration of transmission of carrier-suppressed RZ ASK format transmission over 4 span transmission link with and without one span Raman Optical Amplifiers are shown in Figure 52. At one unit of the quality factor is shown when one Raman OA is incorporated in one span.

8 Concluding remarks

By numerically solving the set of ODEs for pump and signal power and noises in both distributed and discrete ROA, the design concerns of gain, NF and dispersion were examined.

Distributed amplification was shown to pump for 100km spans of different commercial fibers. The required power for each fiber for net gain to compensate for fiber losses were examined, with pump lasers typical operating at 500mW it showed that the transmission span length for Corning NS-DSF and Truewave could be well extended beyond 100km in a purely distributed ROA.

Typically SMF transmission spans of 50km are used because the NF is close to that of an ideal distributed NF, that is, if the loss is corrected at every point along the fiber. In 100km long spans of fiber, the NF for distributed ROA in comparison to lumped amplifiers is improved by between 6-16dB depending upon the configuration. It was determined that fibers with higher values of g_R provide lower system NFs. Forward pumping achieves a NF improvement of nearly 10dB in comparison to backward pumping. It can be further improved by using a hybrid configuration, such as an EDFA to provide a fraction of the gain to the signal. It increases the overall net gain along the fiber and lowers the required pump power for ROA.

Dispersion was also determined and showed that for the different types of fibers there is no real benefit, however in using different pumping configurations the total non-linear phase shift along the fiber could be reduced. There is an approximate benefit of about 12.5dB in using a backward-pumping configuration.

For discrete Raman amplifiers, typically less than 25km high gains of up to 40dB, could be achieved using specially designed Raman fiber or DCF with high Raman gain efficiencies and small affective areas. The comparison of NF in discrete Raman amplifiers showed for different pumping schemes larger span transmissions resulted in a greater discrepancy of up to 7dB. It was also determined that larger gain efficiencies cause less net gain and more gain saturation to occur.

The parameters of the distributed optical gain and NF were integrated into a Gaussian pulse and propagated down the fiber using the SSFM to convert the average powers of the numerical solutions to pulses. This was achieved by changing the half-step SSFM parameter to include ROA by adding the on-off Raman gain gradient at each step size along the fiber. The associated NFs were added to the system as a discrete value. They were then able to be analysis using the SIMULINK modulation models.

Furthermore the most reliable form of pumping in a system model setting was definitely bi-directional. This pumping scheme finds the trade off between the generated noise and additional nonlinear phase noise effects. The overall distance in which the

signal can propagate without regeneration was found to be 2000 km. The accuracy of this figure depends on many factors. These factors include the SSFM, the sampling of gradients, accuracy of results, dependency upon other programs, runtime of programs etc. Such factors not only affect the distance found, but many of the other eye diagrams and performance quality.

We have shown that through estimation and simulation there can be an accurate depiction of Raman amplification in optical fiber, namely distributed, as it utilizes the fiber in which the signal propagates, to perform the amplification.

Experimental results have also indicated that one unit of the quality factor can be achieved with only one span pumped with a Raman amplifying laser.

9. References

- [1] Headley, C & Agrawal, G P. *Raman Amplification in Fibre Optical Communication Systems*. Elsevier Inc. 2005.
- [2] Islam, M N. *Raman Amplifiers for Telecommunications 1-Physical Principles*. Springer-Verlag Inc. 2004
- [3] Agrawal, G P. *Fiber-Optic Communications Systems, 3rd Ed*. John Wiley & Sons, Inc. 2002
- [4] Kelley, P L. *Nonlinear Fiber Optics 3rd Ed*. Academic Press, 1995
- [5] Daniel J. Blumenthal, “ *Distributed Raman Amplification for Ultra-High Speed Fiber Cross-Phase-Modulation Wavelength Converters* Project Report 2001-02
- [6] Yasuhiro, Aoki *Properties of Fiber Raman Amplifiers and Their Applicability to Digital Optical Communication Systems*. IEEE J. of Lightwave Tech., vol. 6, 1988
- [7] Dakss, Mark L, and Melman, P. *Amplified Spontaneous Raman Scattering and Gain Fiber Raman Amplifiers*. J. of Lightw. Tech., vol. 6. 1985
- [8] Mourad, M, and Acs. *Cross-Gain Modulation in Raman Fiber Amplifier: Experimentation and Modelling*. Photonics Tech Let, Vol 14. 2002
- [9] Bromage, J. *Raman Amplification for Fiber Communications Systems*. IEEE J. Lightw. Tech., vol. 6. 2004
- [10] Namiki, S, and Emori, Y. *Ultrabroad-Band Raman Amplifiers Pumped and Gain-Equalized by Wavelength- Division-Multiplexed High-Power Laser Diodes*, IEEE J. Quant. Elect., Vol 7., 2001
- [11] Stolen, R H. *Relation between the effective area of a single-mode fiber and the capture fraction of spontaneous Raman scattering*. Technical Report, Dep. of Electrical and Computer Engineering, Virginia. USA.
- [12] Suzuki, H and Acs. *Super-Dense WDM Transmission Technology in the Zero-Dispersion Region Employing Distributed Raman Amplification.*, IEEE J. Lightw. Tech, vol. 4, 2003
- [13] D. Dahan and G. Eisenstein, *The properties of amplified spontaneous emission noise in*

- saturated fiber Raman amplifiers operating with CW signals*, Opt. Comm., vol. 236, pp.279-288, 2004.
- [14] Gallion, P, and Acs. *Study of noise properties in optical distributed Raman amplifiers using a semiclassical model*, SPIE, Photonics West, Optoelectronics. San Jose (USA), Jan 2002.
- [15] Wesson, A. V, and Killey, R. I *Calculation of the effect of pump depletion in WDM systems with distributed Raman gain*, Technical report, Dep. of Elect. Eng., University College London
- [16] Xueming, L. "*Optimization for various schemes of distributed fibre Raman amplifiers*", J. Optics A, Vol 6. 2004.